Potential Antitumor Agents. 29. Quantitative Structure–Activity Relationships for the Antileukemic Bisquaternary Ammonium Heterocycles

William A. Denny, Graham J. Atwell, Bruce C. Baguley, and Bruce F. Cain*

New Zealand Cancer Society's Experimental Chemotherapy Research Laboratory, Auckland, New Zealand.
Received May 18, 1978

Quantitative relationships between physicochemical drug properties and antileukemic (L1210) efficacy have been examined for a series of bisquaternary ammonium heterocycles employing multiple variable regression analysis. Three measures of biologic response were examined: ILS_{max}, the percentage increase in mean life span of leukemic animals at the LD_{10} dose; D_{40}, the drug dose necessary to provide 40% increase in life span; and CI ($=LD_{10}/D_{40}$), the chemotherapeutic index. A cross correlation matrix between these three measures and the LD_{10} values demonstrates ILS_{max} and CI to be independent of toxicity. D_{40} is highly inversely correlated with LD_{10} and positively correlated with ILS_{max}, suggesting that this parameter measures a composite of both drug selectivity and toxicity. Superior regression equations resulted at all stages employing ILS_{max} as a measure of antitumor selectivity. Acceptable equations modeling LD_{10} could not be obtained. There was a parabolic relationship between agent lipophilic–hydrophilic balance, measured as chromatographic R_m values, and ILS_{max}. To reduce residual variance in the L1210 screening data, not accepted by this parabolic equation, measures of agent–DNA interaction were investigated as possible indices of site fit. Relative levels of drug–DNA interaction were obtained by spectrofluorimetric quantitation of drug displacement of DNA-bound ethidium. Addition to regression equations of agent C_{50} values for calf thymus DNA, those micromolar drug concentrations necessary to displace 50% of the ethidium bound to that DNA, provided a significant reduction in the screening data variance. C_{50} values for drug interactions with poly[d(A-T)] and poly[d(G·C)] were also investigated as possible indicators of drug selectivity toward different DNA sites. Marked differences were observed in the C_{50} values for the two synthetic nucleic acids, with those for calf thymus DNA and poly[d(G-C)] proving highly covariant. A regression equation containing a positive term in C_{50}[poly[d(G-C)]] and a negative term in C_{50}[poly[d(A-T)]] provided the greatest acceptance of the variation in the biologic data. The term in C_{50}[poly[d(A-T)]] is the single most important equation term, alone accounting for 35% of the variance in the data. This best equation provides both an adequate summary of the L1210 screening data for the 174 active compounds considered and a physical explanation for the antitumor selectivity for these agents. The major factor influencing antitumor selectivity in these drugs is their ability to distinguish alternating adenine-thymine sequences in DNA.

Following demonstration of significant antitumor (L1210) activity with a bisquaternary ammonium heterocycle,[1] a large number of congeners have been synthesized and screened as part of this laboratory's program to develop new antitumor agents.[1-9] This particular series of compounds is remarkable for both the high percentage which prove L1210 active and the extremely high experimental activity shown by certain members. For one example, **221** (Table I, NSC176319), pharmacologic and toxicologic examination has been completed as a prelude to clinical trial.

Employing as a measure of antitumor efficacy the percentage increase in mean life span (ILS), in L1210 screening tests, qualitative structure–activity relationships (SAR) have been developed.[6] The rise and then fall in antileukemic activity, seen on homologation within series of bisquaternary salts (e.g., **89–93** and **100–103**; Table I), suggest that agent lipophilic–hydrophilic balance plays a dominant role in antitumor selectivity. Additionally, certain structural requirements necessary for activity are evident. These include the following: limitations on the separation of the two cationic charges; a need for a close approach to overall planarity, coupled with a certain degree of molecular rigidity;[9] and a molecular outline permitting binding to an annular site limited by radii of 20 and 25 Å.[6] All these features appear compatible with the hypothesis that the minor groove of twin-helical DNA provides the site of drug action.[6]

When derivation of quantitative SAR for these agents is attempted, the marked diversity of structural types precludes the use of usual extrathermodynamic parameters that are appropriate with series of simply substituted drug congeners. From the viewpoint that DNA is a likely site of action for these agents, drug–DNA association constants should then provide measures of site fit and therefore be directly incorporable into correlation equations. Relative drug–DNA binding constants have been measured utilizing drug competition with ethidium for DNA sites. The possible utility of these constants in regression analysis of L1210 screening data for the bisquaternary salts is examined in this study.

Chemistry. With the exception of the acridine congeners, synthesis of the quoted bisquaternary salts employed terminal quaternization of the necessary heterocyclic bisbases. In most cases construction of the bisbase required essentially the assembly of a polyamide framework. For ease of handling of intermediates, attention is drawn to our earlier comments[2] on the high crystallinity and ease of purification of the methyl esters of acid components, in contrast with the sometimes difficultly purifiable, microcrystalline acids.

In cases where the terminal base units were identical and there was a central diacid component (e.g., **303** and **306**; Table II), reaction of the acid chloride from the diacid, with the necessary amine-bearing base unit, as before[1-4] provided the necessary bisbase in essentially quantitative yield. With asymmetric bisbases, stepwise construction of the amide skeleton was necessary and the phosphorazo reaction[2,10] was the one of choice for coupling acid and amine components. In the asymmetric bisbases containing a 4-aminoquinoline unit this component was appended terminally. Quaternization, except when there was marked steric shielding of the ring nitrogen to be alkylated, employed the reaction conditions and precautions detailed earlier.[8] Formerly 8-substituted quinolines such as **307** and **309** proved difficult to completely quaternize.[7] In subsequent work it appeared that one factor contributing to incomplete quaternization was the continually slow breakdown of the initially formed quaternary salt and also the quaternizing agent during the extended reaction times necessary with these sterically hindered bases, acidic byproducts being formed. The salts resulting from these acidic products and the input bisbase were much more slowly quaternized. By carrying out such reactions in the presence of 2 mol equiv of *N,N*-diisopropylethylamine,[11]

0022-2623/79/1822-0134$01.00/0

acid byproducts were scavenged and more complete quaternization resulted.

When terminal reduction of nitro groups was necessary, use of Fe/H^+, as detailed before,[2] provided high yields of the corresponding amines without appreciable overreduction involving the heterocyclic quaternary functions.

All congeners of the 3-amino-9-anilino-10-methylacridinium salts were generated by coupling 3-(trifluoroacetamido)-9-chloro-10-methylacridinium chloride[12] with the requisite aniline component. Hydrolytic removal of the protecting trifluoroacetyl group employed 4 N NH_3 in a suitable solvent.

1,4-Bis(4-nirostyryl)benzene, conveniently prepared in moderate quantities by condensation of (4-nitrophenyl)acetic acid and terephthal dicarboxaldehyde, could be readily reduced ($SnCl_2$–HCl–HOAc) to the corresponding diamine. Application of Zincke's pyridinium salt synthesis,[13] interacting *N*-(2,4-dinitrophenyl)pyridinium 4-toluenesulfonate and 1,4-bis(4-aminostyryl)benzene, readily afforded agent **299**.

Lipophilic–Hydrophilic Balance. The most usually employed measure of such balance is the logarithm of the partition coefficient (P) of the agents in 1-octanol–water. Agent R_m values [$R_m = \log (1/R_f - 1)$], obtained from partition chromatography employing a particular solvent system, are linearly related to log P values in that solvent system. From Hansch's study[14] of the interrelationships between the partition coefficients obtained when different solvents are employed, it is possible to select those solvents which should provide R_m values highly covariant with log P_{oct} values. In particular, with very hydrophilic compounds such as the quaternary salts discussed here, R_m values are considerably more readily measured than log P_{oct} values. By employing a range of neutral compounds, whose log P_{oct} values had been previously measured[14] and provided an acceptable spread and range (−2.92 to 1.64), R_m values in the partition chromatographic system employed were found linearly related to those log P values by the equation

$$\log P = 2.41(\pm 0.34)R_m - 1.31(\pm 0.24) \quad (1)$$

$$n = 25,\ r = 0.95,\ s = 0.15,\ F_{1,23} = 205$$

C_{50} Values for Drug–DNA Interaction. Earlier we reported the development of a method of obtaining measures of the relative DNA-binding level of intercalating agents by spectrofluorimetric quantitation of drug displacement of DNA-bound ethidium.[15,16] The micromolar concentration of drug necessary to displace 50% of the ethidium from DNA sites (C_{50} value) can be shown inversely proportional to the drug–DNA association constant.[16] The ethidium displacement technique provides a readily reproducible, rapid measure of relative DNA binding and requires only milligram quantities of agent and micrograms of DNA. This technique is therefore eminently suitable for rapid examination of a large series of agents such as in the present study. While accurate measures of drug–DNA association constants can be obtained for intercalating agents,[16] it must be emphasized that the bulk of the bisquaternary salts considered here does not bind by intercalation. Examination of representative examples (e.g., **152**, **216**, **221** and **229**; Table I) shows that these provide no unwinding of PM2 bacteriophage DNA by hydrodynamic criteria.[17] Since these agents appear to bind equally well to the DNA of T_2 bacteriophage, in which the major groove is occluded by bulky glycosyl residues,[18] as to other DNA samples of comparable base-pair composition, it appears that they also do not bind in the major groove of the nucleic acid.[19] Lodgment of the bisquaternary salts in the DNA minor groove is compatible with both these observations and the earlier developed qualitative SAR.

Competition between the intercalating agent ethidium and a bisquaternary salt, for DNA, then utilizes two different site types. On intercalation into DNA, ethidium produces distortion in the helical structure and the phenyl ring at the 9 position of this drug protrudes into the minor groove.[20] A bisquaternary salt lodged in the minor groove of a DNA sample prevents ethidium approach to the occluded intercalation sites. Site sizes for the two agent types also differ. Ethidium lodges between two adjacent base pairs and effectively prevents entry of further intercalating molecules into the nearest neighboring potential sites.[21] From model fitting, examples of the bisquaternary salts in the minor groove could mask potential intercalation sites between from three up to seven base pairs. There is no simple proportionality between C_{50} values and association constants which is applicable to the full range of bisquaternary salts. By employing considerably more detailed and laborious techniques, ethidium displacement can provide DNA association constants for members of the bisquaternary salt series.[19] However, for the purposes of this study C_{50} values are best considered as semiempirical parameters defined by and derived from drug–ethidium competition for DNA samples.

The antibiotic distamycin has also been more recently suggested to lodge in the minor groove of DNA samples.[22] The penchant for this antibiotic to bind to adenine-thymine (A-T) rich DNA samples, as shown by more usual binding methods,[22] can be also demonstrated by measuring C_{50} values for the agent, employing as substrates synthetic, homopolymeric DNA samples of defined base-pair sequence (Table I).

Measures of Biologic Response. A prerequisite for regression analysis of biologic data is that the measures be of acceptable form. Two alternate measures of response are considered acceptable: (a) that obtained at a constant dose and (b) that dose necessary to provide a constant biologic response.[23] The latter alternative is almost invariably considered when pharmacodynamic agents are under examination. The desired end point of such research is usually the development of more dose-potent material; the smaller the dose of agent necessary to provide the required response the more active the agent is considered. The needs of the research inevitably dictate the nature of the response measure employed. In contrast, with cancer, and to a certain extent with antiparasitic chemotherapy, more selective agents are sought, those which will provide greater therapeutic responses at permissible doses. Dose potency is of secondary importance. We suggest that in such cases the most important, and pertinent, end point for use in regression analyses is response at a constant dose. Further, when data from animal assays are employed, the "constant" dose must be considered in biologic terms rather than in absolute magnitude, i.e., in terms of toxicity to the animals employed. From this viewpoint a constant dose to animals would be a standard fraction of the LD_{10} or LD_{50} dose. We have recently conducted regression analyses of screening data for several groups of cancer chemotherapeutic agents,[1,24] employing as input the percentage increases in life span [ILS = 100[(T − C)/C]] obtained in L1210 leukemia assays. From a full dose profile of antileukemic activity significant life extensions observed at and below the measured LD_{10} dose were linearly correlated with the logarithms of the corresponding doses. The ILS specified by the linear correlation at the LD_{10} dose (ILS_{max}) was utilized as a measure of antileukemic activity and as input for regression analyses.

Table I

entry no.	type no.	substituent groups R	R¹	R²	R³	link groups A	B	C	counterion[a]	R_m[b]	C_{50} data[c] ct[d]	d(A-T)[e]	d(G-C)[f]	LD_{10}[g]	D_{40}[h]	log ILS_{max}[i] obsd	calcd[j]	diff
54[k]	1	CH_3	H			NHCO	CH	CONH	TsO^-	−0.21				5	*l*	<1.4	<1.4	
55[k]	1	CH_2CH_3	H			NHCO	CH	CONH	TsO^-	0.03				4	*l*	1.43	1.58	-0.15
56[k]	1	$(CH_2)_2CH_3$	H			NHCO	CH	CONH	TsO^-	0.3				21	15	1.89	1.88	0.01
57[k]	1	$(CH_2)_3CH_3$	H			NHCO	CH	CONH	TsO^-	0.67				59	25	2.04	1.81	0.23
58[k]	1	$(CH_2)_4CH_3$	H			NHCO	CH	CONH	TsO^-	0.92				57	55	1.62	1.46	0.16
59[k]	1	$(CH_2)_5CH_3$	H			NHCO	CH	CONH	TsO^-	1.03				27	*l*	<1.4	<1.4	
60[k]	1	$(CH_2)_2OCH_3$	H			NHCO	CH	CONH	TsO^-	0.40				17	11	2.04	1.92	0.13
61[k]	1	$(CH_2)_2OEt$	H			NHCO	CH	CONH	TsO^-	0.8				20	*l*	<1.4	1.67	>-0.27
62[k]	1	$(CH_2)_2OBu$	H			NHCO	CH	CONH	TsO^-	0.94				24	*l*	<1.4	1.42	>-0.02
63[k]	1	CH_2CH_3	NH_2			NHCO	CH	CONH	TsO^-	−0.01				6	*l*	<1.4	1.51	>-0.11
64[k]	1	$(CH_2)_2CH_3$	NH_2			NHCO	CH	CONH	TsO^-	0.25				10	3.9	1.92	1.85	0.07
65[k]	1	$(CH_2)_3CH_3$	NH_2			NHCO	CH	CONH	TsO^-	0.60				18	9	1.72	1.87	-0.15
66[k]	1	$(CH_2)_4CH_3$	NH_2			NHCO	CH	CONH	TsO^-	0.85				16	15	1.51	1.58	-0.07
67[k]	1	CH_3	H			NHCO	CH	CH=CHCONH	TsO^-	−0.2				3	*l*	<1.4	<1.4	
68[k]	1	CH_2CH_3	H			NHCO	CH	CH=CHCONH	TsO^-	0.11				9	5	1.70	1.69	0.01
69[k]	1	$(CH_2)_2CH_3$	H			NHCO	CH	CH=CHCONH	TsO^-	0.50				20	4.3	2.00	1.91	0.09
70[k]	1	$(CH_2)_3CH_3$	H			NHCO	CH	CH=CHCONH	TsO^-	0.9				25	25	1.40	1.50	-0.10
71[k]	1	CH_3	H			NHCO	CH	OCH_2-CONH	TsO^-	-0.3				0.6	*l*	<1.4	<1.4	
72[k]	1	CH_2CH_3	H			NHCO	CH	OCH_2-CONH	TsO^-	−0.11				4	4	1.40	<1.4	
73[k]	1	$(CH_2)_2CH_3$	H			NHCO	CH	OCH_2-CONH	TsO^-	0.15				8.3	6.3	1.59	1.75	-0.16
74[k]	1	$(CH_2)_3CH_3$	H			NHCO	CH	OCH_2-CONH	TsO^-	0.41				210	80	1.96	1.91	0.05
75[k]	1	$(CH_2)_4CH_3$	H			NHCO	CH	OCH_2-CONH	TsO^-	0.78				150	100	1.53	1.69	-0.16
76[k]	1	CH_3	H			NHCO	CH	$(CH_2)_2$-CONH	TsO^-	0.85				270	*l*	<1.4	1.58	>-0.18
77[k]	1	CH_2CH_3	H			NHCO	CH	$(CH_2)_2$-CONH	TsO^-	1.10				1.6	*l*	<1.4	<1.4	
78[k]	1	$(CH_2)_2CH_3$	H			NHCO	CH	$(CH_2)_2$-CONH	TsO^-	1.25				2.0	*l*	<1.4	<1.4	
79[k]	1	CH_3	H			$NHCOCH_2$	CH	CH_2CONH	TsO^-	0.07				15	*l*	<1.4	1.64	>-0.24
80[k]	1	$(CH_2)_3CH_3$	H			$NHCOCH_2$	CH	CH_2CONH	TsO^-	0.92				1.0	*l*	<1.4	1.50	>-0.10
81[m]	1	CH_2CH_3	H			NHCO	CH	NHCO	TsO^-	0.02				4	*l*	<1.4	1.56	>-0.16
82[m]	1	$(CH_2)_3CH_3$	H			NHCO	CH	NHCO	TsO^-	0.59				200	*l*	<1.4	1.87	>-0.47
83[m]	1	$(CH_2)_5CH_3$	H			NHCO	CH	NHCO	TsO^-	1.10				300	*l*	<1.4	<1.4	
84[k]	1	CH_3	H			NHCO	N	CONH	TsO^-	−0.4				4.0	*l*	<1.4	<1.4	
85[k]	1	CH_2CH_3	H			NHCO	N	CONH	TsO^-	−0.15				6.0	6.0	1.42	<1.4	<-0.02
86[k]	1	$(CH_2)_2CH_3$	H			NHCO	N	CONH	TsO^-	0.05				16	14	1.51	1.61	-0.01
87[k]	1	$(CH_2)_3CH_3$	H			NHCO	N	CONH	TsO^-	0.31				175	120	1.87	1.88	-0.01
88[k]	1	$(CH_2)_4CH_3$	H			NHCO	N	CONH	TsO^-	0.60				250	*l*	<1.4	1.87	>-0.46
89[m]	2	CH_3				CONH			TsO^-	−0.25	(0.74)[n]	(0.62)[n]	(1.48)[n]	27	12	2.03	2.06	-0.03
90[m]	2	CH_2CH_3				CONH			TsO^-	0.09	0.74	0.62	1.48	9	2.3	2.20	1.99	0.21
91[m]	2	$(CH_2)_2CH_3$				CONH			TsO^-	0.44	(0.74)	(0.62)	(1.48)	20	10.2	2.17	1.82	0.35
92[m]	2	$(CH_2)_3CH_3$				CONH			TsO^-	0.85	(0.74)	(0.62)	(1.48)	32	32	1.60	1.51	0.09
93[m]	2	$(CH_2)_5CH_3$				CONH			TsO^-	1.10	(0.74)	(0.62)	(1.48)	50	*l*	<1.4	<1.4	

94[o]	3	CH_2CH_3		CONH			TsO^-	−0.12	(2.5)	(2.1)	(4.2)	6	3.1	1.89	1.94	−0.05
95[o]	3	$(CH_2)_3CH_3$		CONH			TsO^-	0.65	2.5	2.1	4.2	19	12	1.72	1.58	0.14
96[m]	4	CH_3		CONH			TsO^-	−0.70	0.37	0.28	0.36	100	39	2.04	1.99	0.05
97[m]	4	CH_2CH_3		CONH			TsO^-	−0.52	(0.37)	(0.28)	(0.36)	45	13	2.05	2.04	0.01
98[m]	4	$(CH_2)_2CH_3$		CONH			TsO^-	−0.21	(0.37)	(0.28)	(0.36)	95	38	1.92	2.04	−0.12
99[m]	4	$(CH_2)_3CH_3$		CONH			TsO^-	0.26	(0.37)	(0.28)	(0.36)	100	41	1.91	1.90	0.01
100[p]	4	CH_3		*q*			TsO^-	−0.52	(0.30)	(0.18)	(0.61)	65	10	1.90	2.17	−0.27
101[p]	4	CH_2CH_3		*q*			TsO^-	−0.10	0.30	0.18	0.61	31	10.5	2.16	2.16	0.00
102[p]	4	$(CH_2)_2CH_3$		*q*			TsO^-	0.49	(0.30)	(0.18)	(0.61)	45	17	2.01	1.92	0.09
103[p]	4	$(CH_2)_3CH_3$		*q*			TsO^-	0.74	(0.30)	(0.18)	(0.61)	57	15	1.73	1.73	0.00
104[m]	5	CH_3		CONH			TsO^-	−0.57	0.30	0.35	0.80	90	80	1.65	2.07	−0.42
105[m]	5	CH_2CH_3		CONH			TsO^-	−0.35	(0.30)	(0.35)	(0.80)	50	35	1.90	2.09	−0.19
106[m]	5	$(CH_2)_2CH_3$		CONH			TsO^-	0.0	(0.30)	(0.35)	(0.80)	80	60	2.08	2.05	0.03
107[p]	6	CH_3		NHCO	CONH		TsO^-	−0.76	0.16	0.16	0.25	34	15	1.85	2.03	−0.18
108[p]	6	CH_2CH_3		NHCO	CONH		TsO^-	−0.40	(0.16)	(0.16)	(0.25)	30	12	2.00	2.10	−0.10
109[p]	6	CH_3		*q*	CONH		TsO^-	−0.57	0.17	0.14	0.28	52	20	1.85	2.11	−0.26
110[p]	6	CH_2CH_3		*q*	CONH		TsO^-	0.08	(0.17)	(0.14)	(0.28)	106	20.4	2.02	2.07	−0.05
111[o]	7	CH_3					TsO^-	0.00	61	63	80	5	*l*	<1.4	1.64	>−0.24
112[m]	8	CH_3					TsO^-	−0.11	11.2	7.7	22	4	*l*	<1.4	1.89	>−0.49
113[m]	8	CH_2CH_3					TsO^-	0.30	(11.2)	(7.7)	(22)	8	*l*	<1.4	1.76	>−0.36
114[m]	8	$(CH_2)_2CH_3$					TsO^-	0.65	(11.2)	(7.7)	(22)	15	*l*	<1.4	1.54	>−0.14
115[m]	9	CH_2CH_3		NHCO	CONH	CONH	TsO^-	−0.44	0.50	0.43	0.65	33	9.1	1.90	2.03	−0.13
116[m]	9	CH_3		NHCO	NHCO	CH=CHCONH	TsO^-	−0.95	0.30	0.22	0.23	100	21	1.99	1.89	0.10
117[m]	9	CH_2CH_3		NHCO	NHCO	CH=CHCONH	TsO^-	−0.58	(0.30)	(0.22)	(0.23)	55	22	1.88	2.01	−0.13
118[m]	9	$(CH_2)_2CH_3$		NHCO	NHCO	CH=CHCONH	TsO^-	−0.20	(0.30)	(0.22)	(0.23)	46	11.5	1.95	2.02	−0.07
119[m]	9	$(CH_2)_3CH_3$		NHCO	NHCO	CH=CHCONH	TsO^-	0.40	(0.30)	(0.22)	(0.23)	24	14	1.72	1.82	−0.10
120[m]	9	CH_3		*q*	NHCO	CONH	TsO^-	−0.40	0.63	0.5	0.84	14	2.5	2.25	2.07	0.18
121[k]	10	CH_3		*q*	NHCO	CONH	TsO^-	−0.75	0.29	0.22	0.37	65	17.9	2.10	2.02	0.08
122[k]	10	CH_2CH_3		*q*	NHCO	CONH	TsO^-	−0.44	(0.29)	(0.22)	(0.37)	43	5.6	2.20	2.09	0.11
123[k]	10	$(CH_2)_2CH_3$		*q*	NHCO	CONH	TsO^-	−0.25	(0.29)	(0.22)	(0.37)	59	4	2.16	2.09	0.07
124[m]	10	CH_3		*q*	NHCO	CH=CHCONH	TsO^-	−0.75	0.3	0.13	0.46	85	26.9	2.16	2.15	0.01
125[m]	10	CH_2CH_3		*q*	NHCO	CH=CHCONH	TsO^-	−0.3	(0.3)	(0.13)	(0.46)	60	5.2	2.25	2.21	0.04
126[m]	10	$(CH_2)_2CH_3$		*q*	NHCO	CH=CHCONH	TsO^-	0.02	(0.3)	(0.13)	(0.46)	20	6.4	2.20	2.16	0.04
127[r]	11	CH_3		NHCO	NHCO	CONH	I^-	−0.12	0.63	0.34	0.97	4.5	0.5	2.12	2.10	0.02
128[r]	12	CH_3		NHCO	NHCO	CONH	I^-	−0.30	0.39	0.27	0.49	19	10	2.00	2.08	−0.08
129[r]	13	CH_3		NHCO	NHCO	CONH	I^-	−0.12	1.38	0.91	2.07	8	0.2	2.18	2.01	0.17
130[s]	14	CH_3		NHCO	NHCO	CONH	TsO^-	−0.77	0.48	0.22	0.64	35	6	2.10	2.08	0.02
131[r]	15	CH_3		NHCO	NHCO	CONH	TsO^-	−0.53	0.46	0.30	0.52	20	8.7	1.93	2.06	−0.13
132[r]	16	CH_3		NHCO	NHCO	CONH	I^-	−0.40	1.14	0.77	1.71	11	1.0	2.20	2.04	0.16
133[r]	17	CH_3		NHCO	NHCO	CONH	I^-	−0.60	0.40	0.26	0.49	20	*l*	<1.4	2.06	>−0.66
134[r]	18	CH_3		NHCO	NHCO	CONH	TsO^-	0.07	0.84	0.44	1.35	9	0.8	2.03	2.04	−0.01
135[o]	19	CH_3		NHCO	NHCO	CONH	I^-	−0.12	0.83	0.79	1.6	17	7.5	2.02	2.02	0.00
136[t]	20	CH_3	CH_3				TsO^-	0.12	11.7	6.0	16.7	40	27	1.79	1.85	−0.06
137[t]	20	CH_2CH_3	CH_3				TsO^-	0.47	(11.7)	(6.0)	(16.7)	18	*q*	<1.4	1.68	>−0.28
138[t]	20	CH_3	OCH_3				TsO^-	−0.41	0.84	0.72	0.9	25	13	1.89	1.97	−0.09
139[t]	20	CH_2CH_3	OCH_3				TsO^-	−0.15	(0.84)	(0.72)	(0.9)	25	10.3	1.86	1.96	−0.10
140[t]	20	$(CH_2)_2CH_3$	OCH_3				TsO^-	0.30	(0.84)	(0.72)	(0.9)	140	140	1.60	1.86	−0.26
141[t]	20	CH_3	Cl				TsO^-	0.36	1.3	1.3	1.5	50	50	1.60	1.73	−0.13
142[s]	21	CH_3	H				TsO^-	0.48	7.8	8.1	14	1.7	*l*	1.43	1.59	−0.16

Table I (*Continued*)

entry no.	type no.	substituent groups R	R¹	R²	R³	link groups A	B	C	counterion[a]	R_m[b]	C_{50} data[c] ct[d]	d(A-T)[e]	d(G-C)[f]	LD_{10}[g]	D_{40}[h]	log ILS_{max}[i] obsd	calcd[j]	diff
143[s]	22	CH_3	H						TsO^-	0.47	6.9	5.4	12	19	14.7	1.65	1.65	0.00
144[s]	23	CH_3	H						TsO^-	0.45	1.5	1.1	2.7	140	54.5	1.84	1.78	0.06
145[u]	24	CH_3	H						TsO^-	0.31	6.8	5.3	11	24	4.3	2.00	1.74	0.26
146[u]	24	CH_2CH_3	H						TsO^-	0.59	(6.8)	(5.3)	(11)	27	18	1.65	1.57	0.08
147[u]	24	$(CH_2)_2CH_3$	H						TsO^-	0.86	(6.8)	(5.3)	(11)	30	*l*	1.54	1.44	0.10
148[r]	25	CH_3	H						TsO^-	0.20	0.9	1.2	1.9	35	25	1.85	1.86	−0.01
149[r]	25	CH_2CH_3	H						TsO^-	0.51	(0.9)	(1.2)	(1.9)	12	12	1.60	1.69	−0.09
150[o]	26	CH_3							TsO^-	0.08	2.2	2.3	2.6	75	72	1.65	1.82	−0.16
151[m]	27	CH_3	H	H	H				TsO^-	−0.74	0.42	0.41	0.91	56	5.9	2.13	2.02	0.11
152[m]	27	CH_2CH_3	H	H	H				TsO^-	−0.32	0.48	0.40	0.90	33	9.8	2.24	2.05	0.19
153[m]	27	$(CH_2)_2CH_3$	H	H	H				TsO^-	0.13	0.44	0.39	0.90	27	12.9	2.06	2.00	0.16
154[m]	27	$(CH_2)_3CH_3$	H	H	H				TsO^-	0.51	0.46	0.41	0.93	58	30	1.76	1.77	0.01
155[m]	27	$(CH_2)_4CH_3$	H	H	H				TsO^-	0.90	0.38	0.42	0.92	70	*l*	<1.4	1.47	>−0.07
156[t]	27	CH_3	H	CH_3	H				TsO^-	0.06	1.2	1.0	2.4	14	5.7	2.09	1.97	0.12
157[t]	27	CH_2CH_3	H	CH_3	H				TsO^-	0.38	(1.2)	(1.0)	(2.4)	26	9.6	1.85	1.83	0.02
158[t]	27	$(CH_2)_2CH_3$	H	CH_3	H				TsO^-	0.75	(1.2)	(1.0)	(2.4)	30	*l*	<1.4	1.57	>−0.17
159[t]	27	CH_3	H	OCH_3	H				TsO^-	0.23	0.64	0.64	1.51	18	10.3	1.72	1.94	−0.22
160[t]	27	CH_2CH_3	H	OCH_3	H				TsO^-	0.55	(0.64)	(0.64)	(1.51)	20	18	1.85	1.76	0.09
161[t]	27	$(CH_2)_2CH_3$	H	OCH_3	H				TsO^-	0.78	(0.64)	(0.64)	(1.51)	22	22	1.60	1.55	0.05
162[t]	27	CH_3	H	NH_2	H				TsO^-	−0.63	0.53	0.37	0.93	20	3.9	2.17	2.05	0.12
163[t]	27	CH_2CH_3	H	NH_2	H				TsO^-	−0.15	(0.53)	(0.37)	(0.93)	14	2.4	2.13	2.09	0.04
164[t]	27	$(CH_2)_2CH_3$	H	NH_2	H				TsO^-	0.20	(0.53)	(0.37)	(0.93)	47	*l*	<1.4	1.99	>−0.59
165[t]	27	CH_3	H	Cl	H				TsO^-	0.05	1.0	0.95	2.0	30	5.6	2.11	1.96	0.15
166[t]	27	CH_2CH_3	H	Cl	H				TsO^-	0.42	(1.0)	(0.95)	(2.0)	29	22	1.70	1.80	−0.10
167[t]	27	$(CH_2)_2CH_3$	H	Cl	H				TsO^-	0.75	(1.0)	(0.95)	(2.0)	40	*l*	<1.4	1.55	>−0.15
168[t]	27	CH_3	NH_2	NH_2	H				TsO^-	−0.7	0.39	0.15	0.54	9	1.4	2.32	2.13	0.19
169[t]	27	CH_3	NH_2	H	NH_2				TsO^-	−0.75	0.26	0.12	0.39	44	2.4	2.35	2.14	0.21
170[t]	27	CH_2CH_3	NH_2	H	NH_2				TsO^-	−0.65	(0.26)	(0.12)	(0.39)	10	3.2	2.18	2.16	0.02
171[t]	27	$(CH_2)_2CH_3$	NH_2	H	NH_2				TsO^-	−0.38	(0.26)	(0.12)	(0.39)	30	5	2.02	2.19	−0.17
172[t]	27	CH_3	OCH_3	H	OCH_3				TsO^-	0.15	0.4	0.30	0.35	41	15	1.78	2.01	−0.23
173[t]	27	CH_2CH_3	OCH_3	H	OCH_3				TsO^-	0.45	(0.4)	(0.30)	(0.35)	40	24	1.76	1.87	−0.11
174[t]	27	$(CH_2)_2CH_3$	OCH_3	H	OCH_3				TsO^-	0.7	(0.4)	(0.30)	(0.35)	37	22	1.79	1.69	0.10
175[t]	27	CH_3	Cl	H	Cl				TsO^-	0.20	1.4	0.99	2.1	26	*l*	<1.4	1.90	>−0.50
176[t]	27	CH_2CH_3	NH_2	NH_2	NH_2				TsO^-	−0.90	(0.26)	(0.08)	(0.48)	14	2.6	2.29	2.14	0.15
177[t]	27	$(CH_2)_2CH_3$	NH_2	NH_2	NH_2				TsO^-	−0.51	0.26	0.08	0.48	10	2.2	2.10	2.27	−0.17
178[r]	28	CH_3	H			NH			TsO^-	0.07	1.30	0.14	1.8	3.1	0.3	2.33	2.30	0.03
179[r]	28	CH_2CH_3	H			NH			TsO^-	0.46	(1.30)	(0.14)	(1.8)	2.5	0.5	2.24	2.11	0.13
180[r]	28	$(CH_2)_2CH_3$	H			NH			TsO^-	0.81	(1.30)	(0.14)	(1.8)	4.1	0.6	1.99	1.84	0.15
181[k]	28	CH_3	H			*q*			TsO^-	−0.3	0.55	0.40	1.15	110	22	2.28	2.11	0.17
182[k]	28	CH_2CH_3	H			*q*			TsO^-	0.09	(0.55)	(0.40)	(1.15)	14	1.2	2.23	2.04	0.19
183[k]	28	$(CH_2)_2CH_3$	H			*q*			TsO^-	0.46	(0.55)	(0.40)	(1.15)	10	4.6	2.03	1.86	0.17
184[p]	29	CH_3	H			NH			I^-	0.06	2.04	0.37	3.01	2.6	0.6	2.28	2.18	0.10
185[o]	30	CH_3	NH_2			NH			TsO^-	0.04	1.5	0.08	1.5	6.7	1.4	2.30	2.39	−0.09
186[o]	30	CH_2CH_3	NH_2			NH			Br^-	0.35	(1.5)	(0.08)	(1.5)	7.5	1.4	2.30	2.26	0.04
187[r]	30	CH_3	H			NH			TsO^-	−0.34	0.43	0.14	0.51	11	4.2	2.28	2.21	0.07
188[r]	30	CH_2CH_3	H			NH			TsO^-	−0.03	(0.43)	(0.14)	(0.51)	8	1.6	2.20	2.17	0.03
189[r]	31	CH_3	H			NH			TsO^-	−0.70	0.31	0.11	0.38	10	5.1	1.88	2.17	−0.29
190[r]	31	CH_2CH_3	H			NH			TsO^-	−0.05	(0.31)	(0.11)	(0.38)	32	9	1.88	2.19	−0.31
191[r]	31	$(CH_2)_2CH_3$	H			NH			Br^-	0.46	(0.31)	(0.11)	(0.38)	25	13	1.85	1.93	−0.12
192[s]	32	CH_3	H			*q*			TsO^-	−0.22	0.83	0.10	0.38	6	1.4	2.34	2.23	0.11
193[u]	33	CH_3	H			NH			Br^-	0.49	42	22	77	30	*l*	<1.4	1.60	>−0.20
194[u]	33	CH_2CH_3	H			NH			ClO_4^-	0.69	(42)	(22)	(77)	20	*l*	<1.4	1.46	>−0.06

195[u]	34	CH_3	H			NH	Br^-	0.59	40	20	75	30	*l*	<1.4	1.55	>−0.15
196[u]	34	CH_2CH_3	H			NH	Br^-	0.83	(40)	(20)	(75)	10	*l*	<1.4	<1.4	
197[r]	35	CH_3				CONH	TsO^-	−0.42	(0.84)	(0.45)	(2.1)	12	1.5	2.22	2.16	0.06
198[r]	35	CH_2CH_3				CONH	TsO^-	−0.19	0.84	0.45	2.1	15	3.5	2.17	2.16	0.01
199[r]	35	$(CH_2)_2CH_3$				CONH	TsO^-	−0.08	(0.84)	(0.45)	(2.1)	50	7	2.15	2.14	0.01
200[o]	35	CH_3				CH=CHCONH	TsO^-	−0.62	0.40	0.11	0.57	50	10.7	2.20	2.24	−0.04
201[o]	35	CH_2CH_3				CH=CHCONH	TsO^-	−0.35	(0.40)	(0.11)	(0.57)	27	5.1	2.23	2.27	−0.04
202[r]	36	CH_3	H				TsO^-	−0.64	0.45	0.29	0.64	75	8.6	2.20	2.07	0.13
203[r]	36	CH_2CH_3	H				TsO^-	−0.3	(0.45)	(0.29)	(0.64)	112	10	2.06	2.10	−0.04
204[r]	36	CH_3	CH_3				TsO^-	−0.71	0.5	0.4	0.8	250	75	2.12	2.02	0.10
205[r]	36	CH_2CH_3	CH_3				TsO^-	−0.4	(0.5)	(0.4)	(0.8)	200	69	2.09	2.07	0.02
206[k]	37	CH_3					TsO^-	0.11	(2.2)	(0.83)	(2.9)	10	*l*	<1.4	1.97	>−0.57
207[k]	37	CH_2CH_3					TsO^-	0.26	(2.2)	(0.83)	(2.9)	10	*l*	<1.4	2.01	>−0.61
208[k]	37	$(CH_2)_2CH_3$					TsO^-	0.40	2.2	0.83	2.9	11	*l*	<1.4	1.87	>−0.47
209[r]	38	CH_3					TsO^-	0.13	5.6	2.8	8.8	16	*l*	<1.4	1.91	>−0.51
210[r]	38	CH_2CH_3					I^-	0.53	(5.6)	(2.8)	(8.8)	16	*l*	<1.4	1.70	>−0.30
211[r]	38	$(CH_2)_2CH_3$					TsO^-	0.71	(5.6)	(2.8)	(8.8)	100	*l*	<1.4	1.57	>−0.17
212[m]	39	CH_3					TsO^-	0.11	*v*	*v*	*v*	7	*l*	<1.4	*w*	
213[m]	39	CH_2CH_3					TsO^-	0.57	*v*	*v*	*v*	13	*l*	<1.4	*w*	
214[m]	39	$(CH_2)_2CH_3$					TsO^-	0.73	*v*	*v*	*v*	100	*l*	<1.4	*w*	
215[r]	40	CH_3					TsO^-	−0.15	0.49	0.15	0.75	25	3.4	2.39	2.23	0.16
216[s]	41	CH_3	H	H	H	CONH	Br^-	0.29	1.4	0.16	3.0	13	2.0	2.23	2.28	−0.05
217[s]	41	CH_2CH_3	H	H	H	CONH	Br^-	0.54	2.0	0.19	3.1	15	2.8	2.07	2.06	−0.01
218[s]	41	$(CH_2)_2CH_3$	H	H	H	CONH	Br^-	0.74	2.3	0.20	3.0	15	8.8	1.81	1.90	−0.09
219[s]	41	$(CH_2)_3CH_3$	H	H	H	CONH	Br^-	1.14	2.1	0.19	2.8	11	*l*	<1.4	1.50	>−0.10
220[x]	41	CH_3	3-CH_3	H	H	CONH	Br^-	0.60	4.9	4.5	15.0	5	*l*	<1.4	1.76	>−0.36
221[x]	41	CH_3	6-NH_2	H	H	CONH	Br^-	0.07	0.66	0.09	1.05	12	1.2	2.35	2.31	0.04
222[x]	41	CH_2CH_3	6-NH_2	H	H	CONH	Br^-	0.22	0.69	0.10	1.04	10	0.9	2.25	2.20	0.05
223[x]	41	$(CH_2)_2CH_3$	6-NH_2	H	H	CONH	Br^-	0.46	0.68	0.10	1.10	10	1.8	2.07	2.11	−0.04
224[x]	41	CH_3	6-Cl	H	H	CONH	TsO^-	0.57	0.79	0.24	1.76	40	14	1.81	1.93	−0.12
225[x]	41	CH_3	6-CH_3	H	H	CONH	TsO^-	0.51	1.05	0.17	2.28	15	1.0	2.17	2.07	0.10
226[x]	41	CH_3	6-OCH_3	H	H	CONH	TsO^-	0.46	0.68	0.19	1.15	50	1.5	2.20	2.00	0.20
227[x]	41	CH_3	7-NH_2	H	H	CONH	Br^-	0.08	0.68	0.23	1.4	11	2	2.11	2.17	−0.06
228[x]	41	CH_3	7-NO_2	H	H	CONH	TsO^-	0.15	0.69	0.20	1.3	27	3	2.02	2.14	−0.12
229[x]	41	CH_3	7-Cl	H	H	CONH	Br^-	0.31	1.0	0.21	2.27	39	12	1.97	2.15	−0.18
230[o]	41	CH_3	8-NH_2	H	H	CONH	I^-	−0.10	0.85	0.20	1.43	60	0.9	2.48	2.25	0.23
231[x]	41	CH_3	8-Cl	H	H	CONH	TsO^-	0.51	1.1	0.29	1.4	55	50	1.70	1.91	−0.21
232[x]	41	CH_3	8-CH_3	H	H	CONH	TsO^-	0.51	0.87	0.31	2.01	60	12	2.02	1.94	0.12
233[x]	41	CH_3	8-OCH_3	H	H	CONH	Br^-	0.30	0.76	0.16	1.62	6	0.3	2.14	2.16	−0.02
234[y]	41	CH_3	3-Ph, 6-NH_2	H	H	CONH	Br^-	0.65	0.39	0.15	0.63	22	10	1.78	1.84	−0.06
235[x]	41	CH_3	H	H	H	NHCO	TsO^-	0.27	1.6	0.21	3.0	7.5	2.2	2.29	2.20	0.09
236[x]	41	CH_2CH_3	H	H	H	NHCO	Br^-	0.45	(1.6)	(0.21)	(3.0)	10	0.6	2.16	2.10	0.06
237[x]	41	CH_3	6-NH_2	H	H	NHCO	TsO^-	0.05	0.60	0.12	1.20	11	1.2	2.30	2.28	0.02
238[x]	41	CH_2CH_3	6-NH_2	H	H	NHCO	I^-	0.19	(0.60)	(0.12)	(1.20)	9	0.7	2.23	2.23	0.00
239[x]	41	CH_3	7-NH_2	H	H	NHCO	TsO^-	−0.04	0.43	0.12	1.04	25	1.5	2.34	2.29	0.05
240[x]	41	CH_3	7-NHCO-CH_3	H	H	NHCO	TsO^-	−0.10	0.34	0.13	0.53	97	10	2.26	2.21	0.05
241[o]	41	CH_3	6-NH_2, 8-OCH_3	H	H	NHCO	TsO^-	0.07	0.31	0.10	0.61	56	1.1	2.33	2.23	0.10
242[x]	41	CH_3	6-NH_2	H	H	NHCONH	TsO^-	0.17	0.51	0.28	1.2	6	3	1.74	2.08	−0.34
243[x]	41	CH_3	H	H	H	CH=CH	Br^-	0.61	0.34	0.13	0.67	23	12	1.89	1.90	−0.01
244[x]	41	CH_3	6-NH_2	H	H	CH=CH	Br^-	0.31	0.38	0.15	0.53	16	1.8	2.19	2.04	0.15
245[x]	41	CH_3	6-NH_2	H	H	$C(CH_3)$=$C(CH_3)$	Cl^-	0.96	1.7	0.9	2.6	5.5	*l*	1.53	1.40	0.13

Table 1 (*Continued*)

entry no.	type no.	substituent groups R	R¹	R²	R³	link groups A	B	C	counterion[a]	R_m[b]	C_{50} data[c] ct[d]	d(A-T)[e]	d(G-C)[f]	LD_{10}[g]	D_{40}[h]	log ILS_{max}[i] obsd	calcd[j]	diff
246[x]	41	CH_3	H	H	H	CH=CHCONH			Br^-	0.28	0.38	0.15	0.71	22	1.3	2.22	2.09	0.13
247[x]	41	CH_3	6-NH_2	H	H	CH=CHCONH			TsO^-	0.03	0.46	0.09	0.41	40	1.6	2.24	2.21	0.03
248[y]	41	CH_3	H	NH_2	H	CONH			I^-	0.24	1.03	0.22	2.9	29	1.1	2.18	2.20	-0.01
249[y]	41	CH_2CH_3	H	NH_2	H	CONH			I^-	0.65	(1.03)	(0.22)	(2.9)	53	11.9	1.95	1.95	0.00
250[y]	41	$(CH_2)_2CH_3$	H	NH_2	H	CONH			I^-	0.71	(1.03)	(0.22)	(2.9)	24	24	1.60	1.84	-0.24
251[y]	41	CH_3	H	H	NH_2	CONH			I^-	0.24	2.25	0.43	4.76	8	2.8	1.85	2.14	-0.29
252[y]	41	CH_2CH_3	H	H	NH_2	CONH			I^-	0.56	(2.25)	(0.43)	(4.76)	10	5.1	1.69	1.95	-0.26
253[y]	41	$(CH_2)_2CH_3$	H	H	NH_2	CONH			I^-	0.76	(2.25)	(0.43)	(4.76)	4.4	*l*	1.43	1.80	-0.37
254[y]	41	CH_3	H	NH_2	NH_2	CONH			I^-	0.08	1.76	0.79	3.17	18	15	1.78	2.04	-0.26
255[y]	41	CH_2CH_3	H	NH_2	NH_2	CONH			I^-	0.35	(1.76)	(0.79)	(3.17)	20	*l*	<1.4	1.92	>-0.52
256[y]	41	$(CH_2)_2CH_3$	H	NH_2	NH_2	CONH			I^-	0.63	(1.76)	(0.79)	(3.17)	15	*l*	<1.4	1.74	> 0.34
257[y]	41	CH_3	6-NH_2	NH_2	H	CONH			I^-	0.01	0.49	0.10	1.1	20	2.9	2.45	2.32	0.13
258[y]	41	CH_2CH_3	6-NH_2	NH_2	H	CONH			I^-	0.37	(0.49)	(0.10)	(1.1)	17	1.4	2.33	2.17	0.16
259[y]	41	$(CH_2)_2CH_3$	6-NH_2	NH_2	H	CONH			I^-	0.52	(0.49)	(0.10)	(1.1)	20	5.9	2.03	2.08	-0.05
260[y]	41	CH_3	6-NH_2	H	NH_2	CONH			I^-	-0.03	0.71	0.23	1.3	3	0.7	2.18	2.19	0.01
261[y]	41	CH_2CH_3	6-NH_2	H	NH_2	CONH			I^-	0.15	(0.71)	(0.23)	(1.3)	6.5	1.5	2.10	2.14	-0.04
262[y]	41	$(CH_2)_2CH_3$	6-NH_2	H	NH_2	CONH			I^-	0.41	(0.71)	(0.23)	(1.3)	10	3.6	1.95	2.01	0.06
263[y]	41	CH_3	7-NH_2	NH_2	H	CONH			Br^-	-0.12	(0.52)	(0.13)	(1.11)	20	1.2	2.45	2.30	0.15
264[y]	41	CH_2CH_3	7-NH_2	NH_2	H	CONH			Br^-	0.07	0.52	0.13	1.11	11	1.4	2.39	2.25	0.14
265[y]	41	CH_3	2-CH_3, 6-NH_2	NH_2	H	CONH			I^-	0.16	(0.50)	(0.31)	(1.17)	110	8.4	2.20	2.06	0.14
266[y]	41	CH_2CH_3	2-CH_3, 6-NH_2	NH_2	H	CONH			I^-	0.34	0.50	0.31	1.17	20	7.2	1.86	1.98	-0.12
267[y]	41	CH_3	H	NH_2	H	NHCO			Br^-	0.35	1.87	0.64	2.05	7	*l*	<1.4	1.91	>-0.51
268[x]	42	CH_3	H	H	H	CONH			TsO^-	0.33	0.89	0.30	3.0	15	2.2	2.08	2.11	0.03
269[x]	42	CH_2CH_3	H	H	H	CONH			TsO^-	0.55	(0.89)	(0.30)	(3.0)	10	2.7	1.98	1.97	0.01
270[x]	42	$(CH_2)_2CH_3$	H	H	H	CONH			Br^-	0.80	(0.89)	(0.30)	(3.0)	4.8	4.8	1.60	1.77	-0.17
271[x]	43	CH_3	H	H	H	CONH			TsO^-	-0.01	1.24	0.22	2.73	20	3.5	2.27	2.29	0.02
272[x]	43	CH_2CH_3	H	H	H	CONH			I^-	0.45	(1.24)	(0.22)	(2.73)	32	3.3	2.11	2.08	0.03
273[x]	43	$(CH_2)_2CH_3$	H	H	H	CONH			I^-	0.68	(1.24)	(0.22)	(2.73)	40	15.8	1.85	1.92	-0.07
274[y]	43	CH_3	6-NH_2	NH_2	H	CONH			TsO^-	0.25	0.62	0.11	1.08	75	4.4	2.41	2.34	0.07
275[y]	43	CH_2CH_3	6-NH_2	NH_2	H	CONH			TsO^-	0.33	(0.62)	(0.11)	(1.08)	100	8.6	2.28	2.17	0.11
276[y]	43	$(CH_2)_2CH_3$	6-NH_2	NH_2	H	CONH			TsO^-	0.56	(0.62)	(0.11)	(1.08)	50	13.7	2.03	2.03	0.00
277[x]	44	CH_3	H	H	H	CONH			TsO^-	-0.07	0.78	0.39	1.04	33	13	1.91	2.08	-0.17
278[x]	44	CH_3	6-NH_2	H	H	CONH			Br^-	-0.45	0.40	0.11	0.50	28	2.1	2.31	2.27	0.04
279[x]	44	CH_3	7-NH_2	H	H	CONH			TsO^-	-0.36	0.53	0.19	1.0	31	4	2.20	2.23	-0.03
280[x]	44	CH_3	7-NO_2	H	H	CONH			Cl^-	-0.24	0.2	0.13	0.74	56	5.9	2.18	2.27	-0.09
281[x]	44	CH_3	6-NH_2	H	H	NHCO			TsO^-	0.1	0.40	0.12	0.52	40	2.6	2.37	2.23	0.14
282[x]	44	CH_3	7-NH_2	H	H	NHCO			Br^-	0.35	0.35	0.17	0.60	165	30	2.28	2.20	0.08
283[x]	44	CH_3	6-NH_2	H	H	NHCONH			Br^-	-0.15	0.42	0.25	0.53	150	18.5	2.20	2.09	0.11
284[y]	44	CH_3	6-NH_2	NH_2	H	CONH			Br^-	-0.41	0.51	0.21	0.78	40	1.7	2.25	2.21	0.04
285[y]	44	CH_2CH_3	6-NH_2	NH_2	H	CONH			TsO^-	0.2	(0.51)	(0.21)	(0.78)	50	6.0	2.32	2.18	0.14
286[y]	44	$(CH_2)_2CH_3$	6-NH_2	NH_2	H	CONH			TsO^-	0.07	(0.51)	(0.21)	(0.78)	60	10	2.20	2.12	0.10
287[o]	45	CH_3	6-NH_2	H	H	NHCO			TsO^-	0.17	0.65	0.35	0.87	7	2	1.90	2.00	-0.10
288[o]	46	CH_3	6-NH_2	H	H	NHCO			TsO^-	-0.47	0.31	0.22	0.34	140	22.1	1.95	2.07	-0.12
289[x]	47	CH_3							TsO^-	0.13	0.88	0.50	1.7	3	*l*	<1.4	2.03	>-0.63
290[y]	48	CH_3	6-NH_2	NH_2	H				TsO^-	-0.15	1.58	0.25	2.68	9	1.1	2.03	2.29	-0.26
291[y]	48	CH_3	6-NH_2	H	NH_2				Br^-	0.3	0.60	0.15	0.91	20	1.0	2.43	2.27	0.16
292[y]	48	CH_3	7-NH_2	H	NH_2				TsO^-	0.12	0.44	0.14	0.77	20	1.7	2.38	2.24	0.14
293[y]	48	CH_3	7-NH_2	OCH_3	H				Br^-	0.14	0.69	0.15	1.18	14	3	2.23	2.21	0.02

294[o]	49	CH_3	3-NH_2	NHCO	Cl^-	0.47	0.11	0.06	0.16	37	2	2.23	2.13	0.10
295[o]	49	CH_3	3-NH_2	$NHSO_2$	ClO_4^-	0.57	0.10	0.07	0.12	35	5	2.18	1.84	0.34
296[o]	50	CH_3	3-NH_2	NHCONH	Cl^-	0.69	0.13	0.09	0.20	22	0.3	2.55	1.76	0.78
297[o]	51	CH_3	3-NH_2	NHCONH	Cl^-	0.46	0.09	0.06	0.13	200	8	2.48	1.95	0.54
298[z]	52	CH_3	2-NH_2	CONH	Cl^-	0.44	0.17	0.09	0.25	55	9	2.36	1.97	0.39
299[o]	53				TsO^-	0.05	0.76	0.20	2.1	7	1.6	1.95	2.25	−0.30
distamycin							0.68	0.07	2.4					

[a] TsO^- = *p*-toluenesulfonate. [b] Relative measure of lipophilic-hydrophilic balance from partition chromatography; see Experimental Section. [c] The C_{50} value is the micromolar drug concentration necessary to displace 50% of DNA-bound ethidium; see Experimental Section and ref 15 and 16. [d] ct = calf thymus DNA. [e] d(A·T) = poly[d(A-T)] – poly[d(A-T)]. [f] d(G-C) = poly[d(G·C)] – poly[d(G-C)]. [g] LD_{10}, lethal dose for 10% of the animals in mg/kg. [h] D_{40}, dose in mg/kg providing 40% increase in the life span of leukemic animals. [i] ILS_{max}, percentage increase in life span in L1210 assays at the LD_{10} dose; see text. [j] Log ILS values for compounds 54–88 were calculated using eq 2 and for compounds 89–299 using eq 23. [k] Reference 1. [l] ILS of 40% not reached at the LD_{10} dose. [m] Reference 2. [n] C_{50} values in parentheses were assumed to be the same as those measured for their homologous counterparts; see text. [o] New compounds; analytical data provided in Table II. [p] Reference 5. [q] Biphenyl link group. [r] Reference 4. [s] Reference 6. [t] Reference 3. [u] Reference 9. [v] Compound too water insoluble to measure C_{50} values. [w] Calculation not possible. [x] Reference 7. [y] Reference 8. [z] Reference 32.

Table II. Structural and Analytical Details for Previously Unreported Bisquaternary Heterocycles

entry	type	substituents				link groups					
no.[a]	no.	R	R^1	R^2	R^3	A	B	C	mp, °C	formula	analyses[b]
300	3	–[c]				CONH			>360	$C_{29}H_{21}N_5O_3$	C, H, N
94	3	CH_2CH_3				CONH			196–198	$C_{33}H_{31}N_5O_3I_2 \cdot 3H_2O$	C, H, N; I[d]
95	3	$(CH_2)_3CH_3$				CONH			265–266	$C_{37}H_{39}N_5O_3I_2$	C, H, I
111	7	CH_3							308–309	$C_{34}H_{34}N_4O_8S_2$[e]	C, H, N, S
301	19	–				NHCO	NHCO	CONH	348–350	$C_{32}H_{24}N_6O_4$	C, H, N
135	19	CH_3				NHCO	NHCO	CONH	317–318	$C_{34}H_{30}N_6O_4I_2$	C, H, I
302	26	–							>360	$C_{36}H_{26}N_6O_4 \cdot 0.5H_2O$	C, H, N
150	26	CH_3							330–331	$C_{52}H_{46}N_6O_{10}S_2 \cdot 0.5H_2O$[e]	C, H, N
303	30	–	NO_2			NH			332–324	$C_{32}H_{24}N_8O_6$	C, H, N
304	30	CH_3	NO_2			NH			192–193	$C_{48}H_{44}N_8O_{12}S_2$[e]	C, H, S
305	30	CH_2CH_3	NO_2			NH			228–230	$C_{36}H_{34}N_8O_6Br_2$	C, H, Br
185	30	CH_3	NH_2			NH			248–250	$C_{48}H_{48}N_8O_8S_2 \cdot 1.5H_2O$	C, H, S
186	30	CH_2CH_3	NH_2			NH			300–301	$C_{36}H_{38}N_8O_2Br_2$	C, H, Br
306	35	–				CH=CHCONH			347–349	$C_{30}H_{26}N_{10}O_2 \cdot 0.5H_2O$	C, H, N
200	35	CH_3				CH=CHCONH			>360	$C_{48}H_{46}N_{10}O_8S_2$[e]	C, H, N, S
201	35	CH_2CH_3				CH=CHCONH			216–218	$C_{48}H_{50}N_{10}O_8S_2 \cdot 1.5H_2O$[e]	C, H, S
307	41	–	8-NO_2	H	H	CONH			274–275	$C_{27}H_{20}N_6O_3 \cdot H_2O$	C, H, N
308	41	CH_3	8-NO_2	H	H	CONH			235–237	$C_{29}H_{26}N_6O_3Br_2$	C, H, N, Br
230	41	CH_3	8-NH_2	H	H	CONH			224–225	$C_{29}H_{28}N_6OI_2$	C, H, N, I
309	41	–	6-NO_2, 8-OCH_3	H	H	NHCO			209–211	$C_{28}H_{22}N_6O_4 \cdot H_2O$	C, H, N
310	41	CH_3	6-NO_2, 8-OCH_3	H	H	NHCO			207–208	$C_{44}H_{42}N_6O_{10}S_2$[e]	C, H, N, S
241	41	CH_3	6-NH_2, 8-OCH_3	H	H	NHCO			176–178	$C_{44}H_{44}N_6O_8S_2 \cdot H_2O$[e]	C, H, N, S
311	45	CH_3	6-NO_2	H	H	NHCO			284–286	$C_{29}H_{28}N_6O_3Cl_2$	C, H, N, Cl
287	45	CH_3	6-NH_2	H	H	NHCO			321–322	$C_{43}H_{43}N_6O_7S_2$[e]	C, H, N, S
312	46	–	6-NO_2	H	H	NHCO			>360	$C_{35}H_{25}N_7O_5 \cdot 0.5H_2O$	C, H; N[f]
313	46	CH_3	6-NO_2	H	H	NHCO			203–205	$C_{51}H_{45}N_7O_{11}S_2 \cdot H_2O$[e]	C, H, N, S
288	46	CH_3	6-NH_2	H	H	NHCO			256–257	$C_{51}H_{47}N_7O_9S_2$[e]	C, H, N, S
294	49	CH_3	3-NH_2			NHCO			277–282	$C_{33}H_{30}N_6OCl_2 \cdot 5H_2O$	C, H, N, Cl
295	49	CH_3	3-NH_2			$NHSO_2$			195–197	$C_{32}H_{30}N_6SO_{10}Cl_2 \cdot H_2O$	C, H, N, Cl
296	50	CH_3	3-NH_2			NHCONH			269 dec	$C_{30}H_{31}N_9OCl_2$	C, H, N, Cl
297	51	CH_3	3-NH_2			NHCONH			306–309	$C_{29}H_{30}N_{10}OCl_2$	C, H, N, Cl
299	53								371–372	$C_{46}H_{40}N_2O_6S_2$[e]	C, H, N, S

[a] Entries below number 300 refer to formerly unreported compounds for which biophysical and biological test data have been provided in Table I. [b] Elementary analyses for the elements indicated gave results within ±0.4% of those required for the formula provided, unless otherwise indicated. [c] (–) denotes no ring nitrogen substituent; that is, details are for the unquaternized parent bisbase. [d] I: calcd, 29.8; found, 31.1. [e] Anion *p*-toluenesulfonate. [f] N: calcd, 15.5; found, 14.8.

Such a data manipulation method utilizes the totality of the screening data, thereby assisting to minimize biologic variation, and also limits acceptance of unrealistic "best ever" ILS values which can result from successful employment of a dose exceeding the LD_{10} or other chance event. Measures of the dose necessary to provide a constant biologic response, for example, that to provide an ILS of 40% (D_{40}), are also available from the linear correlations. The same data processing method has been used in the present work; where necessary to meet the stringencies of this procedure,[24] additional animal test data have been obtained. The agents previously examined[24,25] consisted primarily of homologous series wherein, from current views,[26,27] there should be close to parabolic relationships between measures of agent lipophilic–hydrophilic balance and ILS_{max}. The excellent agreement found between the binomial correlation equations derived and the observed biologic data[24,25] suggests that further investigation of the use of ILS_{max} in regression analysis is clearly warranted.

The present bisquaternary salt series also contains many homologous series and provides an extensive data base (Tables I and II) which would permit further examination of the applicability of our methods. Further, analysis of the large data base using the two alternate types of response assessment—ILS_{max}, representing response at constant toxicity, and D_{40}, a measure of the dose necessary to provide a constant response—might provide information on which particular measure was more appropriate in such studies. An additional measure of drug selectivity, the chemotherapeutic index (LD_{10}/D_{40} = CI), apparently unexamined in regression analyses, is readily available from the screening data and has also been included in this comparative study.

Results and Discussion

Adequate biological test data were available for 246 bisquaternary salts, 198 of which were active and 48 inactive. This data set embraces all active bisquaternary salts previously reported[1-9] and most inactive examples as well. Many of the inactive compounds excluded were nitro group substituted derivatives which were merely prepared as intermediates to the corresponding, extremely active amino compounds[8] and were accordingly not screened. A small number of agents, containing six aromatic rings, proved so exceedingly insoluble that C_{50} values could not be determined. Formerly unreported compounds are listed in Table II. The generic formulas for the agents are **1–53** (Chart I), and all necessary parameter values are provided in Table I.

The first group of compounds in Table I (**54–88**), all represented by formula **1**, includes the 18 active compounds described in the first paper of this series.[1] Certain of these earliest prepared analogues had been completely used in screening so that C_{50} values for all members could not be measured without resynthesis. As the activities of these closely related congeners could be adequately summarized by a simple parabolic equation in R_m alone (eq 2), it was decided that resynthesis would not be

$$\log ILS_{max} = -2.00(\pm 0.64)R_m^2 + 1.77(\pm 0.56)R_m + 1.53 \quad (2)$$

$$n = 18,\ r = 0.86,\ s = 0.14,\ F_{2,15} = 25.6$$

warranted. Attention would instead be concentrated on the remaining examples (**89–293**) which form a better sample set for our aims since there is a considerably greater structural variation in the group and there is a much higher level of data variance which is not accepted by equations in R_m alone (see later). In fact, inclusion of data for compounds **54–88**, for which there is relatively high correlation coefficient for equations in R_m alone, into the total data set might serve to attenuate differences between any alternate regression equations developed.

Table III. Correlation Matrix for Interrelationships of Measures of Activity Employed

	log $(1/D_{40})$	log LD_{10}	log CI
log ILS_{max}	0.597	−0.067	0.780
log $(1/D_{40})$		−0.711	0.696
log LD_{10}			0.011

The remaining major group of 204 agents (**89–293**; Table I) of diverse structure (formulas **2–47**) contained 174 L1210 active examples. Five of these (**142, 147, 245, 250** and **253**) showed levels of activity between 25 and 40% ILS, and, accordingly, D_{40} values for these could not be derived. For the remaining 169 compounds, all three measures of biologic activity of interest were available, and it was clearly desirable to examine the interrelationship of these and the possible correspondence with toxicity as provided by the LD_{10} values. The cross correlation matrix for the logarithms of these four parameters (Table III) supports the contention that ILS_{max} and CI are measures of drug selectivity since the very low coefficients associated with LD_{10} terms suggest that these two factors are unrelated to toxicity. ILS and CI are quite highly correlated. In contrast, D_{40} is highly inversely correlated with toxicity (LD_{10}) and directly correlated with ILS_{max}; it appears that this parameter is a composite of measures of both selectivity and toxicity.

Equations in R_m Alone. Earlier work[6] had demonstrated that the lipophilic–hydrophilic balance of these agents was critical for display of biologic activity. As a rise and then fall in L1210 activity were seen as the alkyl quaternary function, on a particular structural variant, was progressively lengthened, parabolic relationships between R_m and biologic activity were confidently expected. In agreement, equations linking the various measures of biologic activity and R_m values alone (eq 3 and 4) were

$$\log ILS_{max} = -0.24(\pm 0.07)R_m + 2.05 \quad (3)$$

$$n = 174,\ r = 0.45,\ s = 0.21,\ F_{1,172} = 43.2$$

$$\log CI = -0.21(\pm 0.14)R_m + 0.66 \quad (4)$$

$$n = 169,\ r = 0.23,\ s = 0.37,\ F_{1,167} = 9.3$$

$$\log ILS_{max} = -0.44(\pm 0.14)R_m^2 - 0.23(\pm 0.06)R_m + 2.14 \quad (5)$$

$$n = 174,\ r = 0.59,\ s = 0.19,\ F_{2,171} = 46$$

$$\log CI = -0.60(\pm 0.29)R_m^2 - 0.23(\pm 0.13)R_m + 0.76 \quad (6)$$

$$n = 169,\ r = 0.37,\ s = 0.36,\ F_{2,166} = 13.6$$

$$\log (1/D_{40}) = -0.74(\pm 0.42)R_m^2 - 0.02(\pm 0.19)R_m + 5.32 \quad (7)$$

$$n = 169,\ r = 0.26,\ s = 0.53,\ F_{2,166} = 6.0$$

significantly improved by incorporation of terms in R_m^2 (eq 5–7). In fact, the coefficient associated with the R_m term in eq 7 is not appreciably different from zero. No significant equation linking D_{40} or LD_{10} with R_m alone could be computed. Similarly, no parabolic equation in R_m could be derived for LD_{10}. Stepwise development of these various equations is detailed in Table IV.

Even with the best of these equations (eq 5) 65% ($1 - r^2$) of the variance in the biologic data remains unaccounted for.

For the diverse range of structural types in the data base (**89–293**) it is clearly impossible to employ usual extra-

Chart I

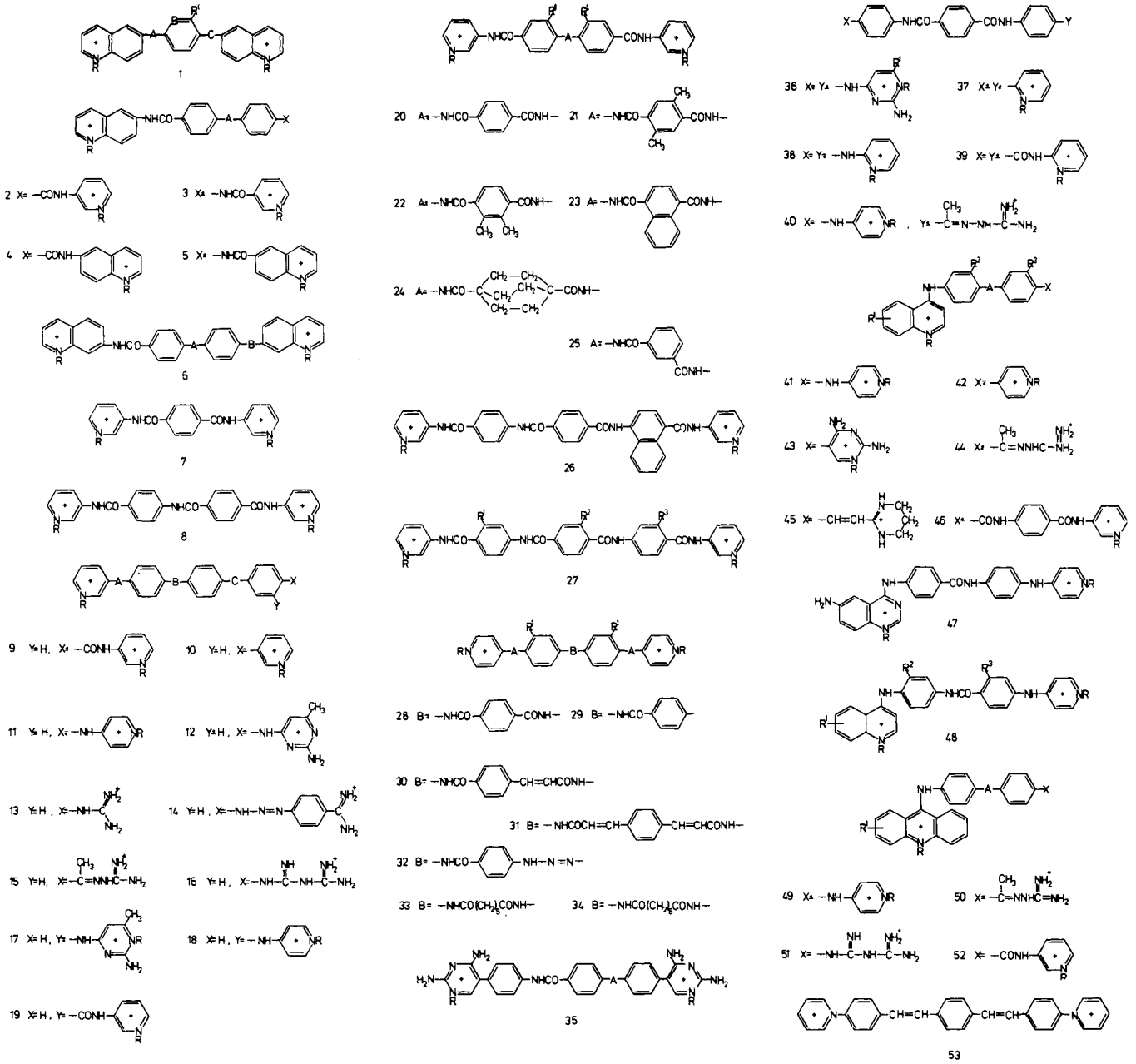

thermodynamic parameters to effectively reduce remaining variance. Use of suitable indicator variables could of course be investigated and might afford equations which would provide a summary of the L1210 data. However, use of such variables would be unlikely to increase our understanding of the physical events associated with drug–tumor–host selectivity. For the reasons detailed earlier we chose to examine C_{50} values for drug displacement of DNA-bound ethidium as an additional variable in regression analyses. Such C_{50} values are inversely related to drug–DNA association constants,[15,16] and the logarithms of such constants are linear free energy related parameters appropriate for use in Hansch analysis.[28] The appropriate form of the C_{50} values to employ in regression equations would then appear to be log $(1/C_{50})$. Following an encouraging preliminary sampling, C_{50} values for drug interaction with calf thymus DNA [C_{50}(ct)] for the range of compounds **89–293** were measured. In two homologous series (**151–155** and **216–219**) the C_{50} values proved essentially constant throughout each; the paraffinic chains attached to the quaternary nitrogen atoms do not themselves appear to contribute significantly to DNA binding. Accordingly, in remaining homologous series C_{50} values were measured for one member and assumed to be the same for other members; such assumed values are provided in parentheses in Table I.

Incorporation of C_{50}(ct) values into regression equations produces a significant reduction in total variance when modeling ILS_{max} (eq 8), the partial F for introduction of

$$\log ILS_{max} = -0.45(\pm0.14)R_m^2 - 0.18(\pm0.07)R_m + 0.11(\pm0.09) \log [1/C_{50}(ct)] + 2.11 \quad (8)$$

$$n = 174,\ r = 0.61,\ s = 0.19,\ F_{3,170} = 33.1$$

$$\log CI = -0.62(\pm0.30)R_m^2 - 0.19(\pm0.14)R_m + 0.11(\pm0.20) \log [1/C_{50}(ct)] + 0.74 \quad (9)$$

$$n = 169,\ r = 0.38,\ s = 0.36,\ F_{3,165} = 9.5$$

$$\log (1/D_{40}) = -0.71(\pm0.41)R_m^2 - 0.20(\pm0.29)R_m - 0.07(\pm0.22) \log [1/C_{50}(ct)] + 5.35 \quad (10)$$

$$n = 169,\ r = 0.28,\ s = 0.52,\ F_{3,165} = 4.8$$

Table IV. Steps in the Development of the Equations Discussed[a]

eq no.	intercept	R_m	R_m^2	ct	r	s	$F_{1,X}$[b]
3	2.05	−0.24			0.45	0.21	43.2 (172)
5	2.14	−0.23	−0.44		0.59	0.19	39.3 (171)
8	2.11	−0.18	−0.45	−0.11	0.61	0.19	5.0 (170)
		R_m^2	R_m	r	s	$F_{1,X}$	
	5.31	−0.74		0.26	0.53	12.1 (167)	
7	5.32	−0.74	−0.02	0.26	0.53	0.2 (166)	
		R_m^2	R_m	ct	r	s	$F_{1,X}$
	0.75	−0.59			0.29	0.38	15.0 (167)
6	0.76	−0.60	−0.22		0.37	0.36	11.9 (166)
9	0.74	−0.62	−0.19	0.11	0.38	0.36	1.2 (165)
		R_m^2	ct	R_m	r	s	$F_{1,X}$
	5.31	−0.74			0.26	0.53	12.1 (167)
	5.34	−0.71	−0.15		0.28	0.52	1.3 (166)
10	5.35	−0.71	−0.20	−0.08	0.28	0.52	0.5 (165)
		A·T	R_m^2	R_m	G·C	r	s	$F_{1,X}$
	1.86	0.34				0.58	0.19	88.0 (172)
	1.94	0.33	−0.44			0.70	0.17	50.6 (171)
	1.97	0.29	−0.43	−0.16		0.76	0.15	35.5 (170)
12	1.88	0.42	−0.39	−0.27	−0.28	0.81	0.14	40.8 (169)
		A·T	R_m^2	R_m	G·C	r	s	$F_{1,X}$
	0.36	0.50				0.47	0.35	47.2 (167)
	0.47	0.51	−0.64			0.56	0.33	23.2 (166)
	0.50	0.47	−0.66	−0.16		0.59	0.32	7.3 (165)
13	0.36	0.69	−0.60	−0.32	−0.43	0.65	0.30	20.0 (164)
		A·T	G·C	R_m^2	R_m	r	s	$F_{1,X}$
	4.91	0.49				0.34	0.51	21.6 (167)
	4.63	0.96	−0.82			0.55	0.46	45.0 (166)
	4.75	0.94	−0.76	−0.63		0.59	0.44	12.3 (165)
14	4.72	0.99	−0.97	−0.062	−0.27	0.62	0.43	8.5 (164)
		R_m	A·T/G·C	R_m^2	r	s	$F_{1,X}$	
3	2.05	−0.24			0.45	0.21	43.2 (172)	
	1.81	−0.35	0.42		0.71	0.16	108.5 (171)	
18	1.90	−0.33	0.39	−0.38	0.79	0.14	50.1 (170)	
		A·T/G·C	R_m	R_m^2	r	s	$F_{1,X}$	
	0.38	0.45			0.37	0.37	27.0 (167)	
	0.28	0.64	−0.41		0.55	0.33	40.3 (166)	
19	0.39	0.62	−0.42	0.56	0.62	0.31	19.3 (165)	
		R_m^2	R_m	A·T/G·C	r	s	$F_{1,X}$	
	2.16	−0.64			0.49	0.23	12.7 (39)	
	2.18	−0.50	−0.24		0.61	0.21	7.4 (38)	
20	1.97	−0.40	−0.36	0.31	0.73	0.18	12.9 (37)	
		R_m^2	R_m	(A)(T)/G·C	r	s	$F_{1,X}$	
	2.16	−0.64			0.49	0.23	12.7 (39)	
	2.18	−0.50	−0.24		0.61	0.21	7.4 (38)	
21	2.09	−0.47	−0.28	0.08	0.62	0.21	1.2 (37)	
		A·T	R_m^2	R_m	G·C	I	r	s	$F_{1,X}$
	1.85	0.35					0.60	0.19	99.2 (177)
	1.94	0.35	−0.42				0.70	0.17	44.6 (176)
	1.96	0.32	−0.40	−0.14			0.74	0.16	25.1 (175)
22	1.90	0.41	−0.37	−0.19	−0.16		0.76	0.15	13.6 (174)
23	1.88	0.42	−0.38	−0.27	−0.27	0.46	0.81	0.14	37.7 (173)

[a] Terms employing C_{50} values for a particular DNA species have been abbreviated; e.g., log $[1/C_{50}(\text{ct})]$ is provided as ct. The same applies for those of the other DNAs employed [A-T; (A)(T); G·C]. [b] The X value pertaining to a particular F test is provided in parentheses.

the third variable being 5.0 although there is only a small increase (0.02) in correlation coefficient. However, when modeling CI and D_{40} such added terms were not significant (eq 9 and 10). Again no significant equation could be derived for LD_{10}. Steps in the development of the above equations are listed in Table IV.

The minor groove of DNA consists essentially of two poly(deoxyribose phosphate) chains. Intuitively it might then be expected that minor-groove binding agents would show similar association constants for all DNA samples of similar topology, regardless of base-pair sequence. Such is clearly not the case. Agents such as distamycin,[22] claimed to bind at this site, show a marked selectivity for adenine·thymine (A-T) rich DNAs when conventional methods of examining binding are employed. C_{50} values for distamycin–ethidium competition for binding sites in poly[d(A·T)] [C_{50}(A·T)] and poly[d(G·C)] [C_{50}(G·C)] clearly display the preference for the A-T rich polymer (Table I). Similarly, examples of the bisquaternary salts provided markedly different [C_{50}(G-C)]/[C_{50}(A-T)] ratios, some examples (e.g., **185** and **216**) providing figures as high as 20. The absolute values of such ratios are of course dependent on the relative binding affinities of ethidium to the two homopolymers; in this case the binding affinities of ethidium to poly[d(A·T)] ($9.5 \pm 0.9 \times 10^6$ M^{-1}) and to poly[d(G·C)] ($9.9 \pm 0.5 \times 10^6$ M^{-1}) are identical within

Table V. Squared Correlation Matrix for the Independent Variables Associated with Equations 12-19

	R_m^2	log $[1/C_{50}$ (ct)]	log $[1/C_{50}$ (A-T)]	log $[1/C_{50}$ (G-C)]	log $[[C_{50}$ (G-C)]/ $[C_{50}$ (A-T)]]
R_m	0.003	0.263	0.059	0.314	0.115
R_m^2		0.001	0.002	0.001	0.005
log $[1/C_{50}$(ct)]			0.464	0.863	0.053
log $[1/C_{50}$(A-T)]				0.401	0.237
log $[1/C_{50}$(G-C)]					0.135

experimental error.[16] Hesitations in accepting the equating of C_{50} values and absolute drug–DNA association constants are of lesser consequence when the ratios $[C_{50}$(G·C)]/$[C_{50}$(A-T)] are considered. Most modifying factors considered, site size, etc., should effectively cancel in such ratios and these should then correlate with the ratio of the drug association constants for the two different DNAs.

Within the DNA of a mammalian cell it is known that certain regions are redundant whereas others, acting as promoters or repressors controlling the synthesis of critical macromolecules, are vital to the continued functioning of the cell.[18] The importance of different regions of DNA to the continued functioning of a cell varies. Drugs capable of distinguishing different regions, i.e., sequences of DNA, are then likely to vary in their ability to disrupt the continued functioning of a cell. It was then clearly of interest to examine if C_{50} values for binding to different DNA samples could be employed to distinguish possibly more drug-sensitive sequences of tumor cells. Accumulated C_{50} values for interaction of the bisquaternary salts with poly[d(A·T)] and poly[d(G·C)] are listed in Table I. The cross correlation matrix relating to use of these values as independent variables in regression equations is provided in Table V.

As seen from this matrix C_{50}(A-T) and C_{50}(G·C) proved to be reasonably independent variables, whereas C_{50}(G-C) and C_{50}(ct) were highly covariant (eq 11).

$$\log [1/C_{50}(\text{ct})] = 0.83(\pm 0.05) \log [1/C_{50}(\text{G·C})] + 0.21 \quad (11)$$

$$n = 174,\ r = 0.93,\ s = 0.14,\ F_{1,172} = 1085$$

By employing the C_{50} values for drug interaction with the two homopolymeric synthetic DNAs, eq 12–14

$$\log \text{ILS}_{max} = -0.39(\pm 0.10)R_m^2 - 0.27(\pm 0.06)R_m + 0.42(\pm 0.07) \log [1/C_{50}(\text{A-T})] - 0.28(\pm 0.08) \log [1/C_{50}(\text{G·C})] + 1.88 \quad (12)$$

$$n = 174,\ r = 0.81,\ s = 0.14,\ F_{4,169} = 81.9,\ R_m(\text{optimum})\ -0.35\ (-0.23 \text{ to } -0.47)$$

$$\log \text{CI} = -0.60(\pm 0.16)R_m^2 - 0.32(\pm 0.13)R_m + 0.69(\pm 0.16) \log [1/C_{50}(\text{A-T})] - 0.43(\pm 0.19) \log [1/C_{50}(\text{G·C})] + 0.36 \quad (13)$$

$$n = 169,\ r = 0.65,\ s = 0.31,\ F_{4,164} = 29.3,\ R_m(\text{optimum})\ -0.27\ (-0.13 \text{ to } -0.41)$$

$$\log (1/D_{40}) = -0.62(\pm 0.36)R_m^2 - 0.27(\pm 0.18)R_m + 0.99(\pm 0.22) \log [1/C_{50}(\text{A-T})] - 0.97(\pm 0.28) \log [1/C_{50}(\text{G-C})] + 4.72 \quad (14)$$

$$n = 169,\ r = 0.62,\ s = 0.43,\ F_{4,164} = 25.5,\ R_m(\text{optimum})\ -0.22\ (-0.03 \text{ to } -0.41)$$

could be derived. Stepwise development of these equations is detailed in Table IV. Again, no significant equation could be derived for LD_{10}.

For all three measures of biologic activity, clearly superior regression equations result on inclusion of C_{50}(A·T) and C_{50}(G·C) values; compare eq 5 and 12, 6 and 13, 7 and 14. Equation 12 highlights the importance of C_{50}(A·T) for antitumor selectivity; the term in this function is the single most important variable, alone accounting for 35% of the variance in the biologic data. Equation 12 provides both a reasonable summary of the experimental data and an explanation of this in physical terms.

Within the confidence limits computed, the coefficients of the terms in C_{50}(A-T) and C_{50}(G·C) in eq 12 are identical and opposite in sign. Rearrangement of eq 12–14 furnishes eq 15–17. Equation 15, employing the ratio of the C_{50} values to the two homopolymers, may be a more satisfactory one than the equivalent eq 12 for several reasons. First, log $[1/C_{50}$(A·T)] is less highly correlated with log $[C_{50}$(G·C)]/$[C_{50}$(A-T)] ($r^2 = 0.237$) than with log $[1/C_{50}$(G·C)] ($r^2 = 0.402$), and the former two variables then better meet desirable criteria for use in regression analysis. Second, it emphasizes the importance of the differential binding of the bisquaternary salts to different DNA sequences in determining the level of biologic activity measured as ILS_{max}. In eq 15 the coefficient associated with the term in $[C_{50}$(G-C)]/$[C_{50}$(A-T)] is of higher significance (computed $T = 6.4$) than that in $1/C_{50}$(A·T) (computed $T = 4.3$). In fact, omission of the latter term from eq 15 provides eq 18 of almost equal usefulness.

$$\log \text{ILS}_{max} = -0.39(\pm 0.10)R_m^2 - 0.27(\pm 0.06)R_m + 0.28(\pm 0.08) \log [[C_{50}(\text{G·C})]/[C_{50}(\text{A-T})]] + 0.15(\pm 0.07) \log [1/C_{50}(\text{A-T})] + 1.88 \quad (15)$$

$$\log \text{CI} = -0.60(\pm 0.16)R_m^2 - 0.32(\pm 0.13)R_m + 0.43(\pm 0.19) \log [[C_{50}(\text{G-C})]/[C_{50}(\text{A-T})]] + 0.26(\pm 0.16) \log [1/C_{50}(\text{A-T})] + 0.36 \quad (16)$$

$$\log (1/D_{40}) = -0.62(\pm 0.36)R_m^2 - 0.27(\pm 0.18)R_m + 0.97(\pm 0.28) \log [[C_{50}(\text{G-C})]/[C_{50}(\text{A·T})]] + 4.72 \quad (17)$$

$$\log \text{ILS}_{max} = -0.38(\pm 0.10)R_m^2 - 0.33(\pm 0.06)R_m + 0.39(\pm 0.07) \log [[C_{50}(\text{G-C})]/[C_{50}(\text{A·T})]] + 1.90 \quad (18)$$

$$n = 174,\ r = 0.79,\ s = 0.14,\ F_{3,170} = 93.4$$

Similarly when the same term is deleted from eq 16, eq 19 results.

$$\log \text{CI} = -0.56(\pm 0.25)R_m^2 - 0.42(\pm 0.12)R_m + 0.62(\pm 0.16) \log [[C_{50}(\text{G-C})]/[C_{50}(\text{A-T})]] + 0.39 \quad (19)$$

$$n = 169,\ r = 0.62,\ s = 0.31,\ F_{3,165} = 33.7$$

Equation 18 also provides a novel perspective—it suggests that the absolute magnitude of DNA binding may be of minor importance; it is the ability of the drugs to distinguish particular DNA sequences which is the critical feature. Other DNA binding drugs, particularly cancer chemotherapeutic agents, might repay investigation employing this perspective. As noted earlier, when ratios of C_{50} values are successfully employed, as in eq 18, there is less concern about the influence of changing site size on C_{50} values as molecular dimensions of the agents change.

Within a subset of 43 compounds, selected to include representatives of the major structural classes and hopefully as representative of the whole data base as possible, C_{50} values for a further synthetic homopolymeric DNA, poly[d(A)]-poly[d(T)] [(A)(T)], were measured. The C_{50} values for the compounds of the subset to all four DNA polymers are listed in Table VI. As a check that these

Table VI. DNA Interaction Data for a Subset of the Bisquaternary Salts

compd no.	C_{50}(ct)[a]	C_{50}(A·T)[b]	C_{50}(G·C)[c]	C_{50}(A)(T)
100	(0.30)[d]	(0.18)[d]	(0.61)[d]	(0.075)[d]
101	0.30	0.18	0.61	0.075
102	(0.30)	(0.18)	(0.61)	(0.075)
103	(0.30)	(0.18)	(0.61)	(0.075)
111	61	63	80	3.8
112	11.2	7.7	22	0.325
121	0.29	0.22	0.37	0.16
122	(0.29)	(0.22)	(0.37)	(0.16)
123	(0.29)	(0.22)	(0.37)	(0.16)
136	11.7	6.0	16.7	0.35
145	6.8	5.3	11	1.6
146	(6.8)	(5.3)	(11)	(1.6)
151	0.42	0.41	0.91	0.13
152	0.48	0.40	0.90	0.11
153	0.44	0.39	0.90	0.12
154	0.46	0.41	0.93	0.14
172	0.40	0.30	0.35	0.18
173	(0.40)	(0.30)	(0.35)	(0.18)
174	(0.40)	(0.30)	(0.35)	(0.18)
178	1.30	0.14	1.8	0.043
179	(1.30)	(0.14)	(1.8)	(0.043)
180	(1.30)	(0.14)	(1.8)	(0.043)
209	5.6	2.8	8.8	0.15
216	1.4	0.16	3.0	0.036
217	(1.4)	(0.16)	(3.0)	(0.036)
218	(1.4)	(0.16)	(3.0)	(0.036)
221	0.66	0.09	1.05	0.048
222	(0.66)	(0.09)	(1.05)	(0.048)
223	(0.66)	(0.09)	(1.05)	(0.048)
230	0.85	0.20	1.43	0.056
231	1.1	0.29	1.4	0.038
251	2.25	0.43	4.76	0.052
252	(2.25)	(0.43)	(4.76)	(0.052)
253	(2.25)	(0.43)	(4.76)	(0.052)
254	1.76	0.79	3.17	0.12
257	0.49	0.10	1.1	0.039
258	(0.49)	(0.10)	(1.1)	(0.039)
259	(0.49)	(0.10)	(1.1)	(0.039)
260	0.71	0.23	1.3	0.067
261	(0.71)	(0.23)	(1.3)	(0.067)
262	(0.71)	(0.23)	(1.3)	(0.067)
264	0.52	0.13	1.11	0.054
281	0.40	0.16	0.52	0.057

[a] See footnote *d*, Table I. [b] See footnote *e*, Table I. [c] See footnote *f*, Table I. [d] See footnote *n*, Table I.

Table VII. Correlation Matrix for the Activity Parameters of the Entries of Table VI

	log $(1/D_{40})$	log LD_{10}	log CI
log ILS_{max}	0.675	−0.111	0.805
log $(1/D_{40})$		−0.761	0.707
log LD_{10}			−0.093

43 agents did provide a representative subset, cross correlation matrices for the biologic parameters (Table VII) and the independent variables (Table VIII) were constructed.

Comparison of the values in Table VII and VIII with those of Tables III and V shows that essentially similar relationships exist between the parameters considered. Similar germinal steps to those followed earlier provide regression eq 20 for these 43 compounds, which can be

$$\log ILS_{max} = -0.40(\pm 0.31)R_m^2 - 0.36(\pm 0.16)R_m + 0.31(\pm 0.19) \log [[C_{50}(G\cdot C)]/[C_{50}(A\cdot T)]] + 1.97 \quad (20)$$

$$n = 41,\ r = 0.73,\ s = 0.18,\ F_{3,37} = 14.0$$

directly compared with that derived from the full data base (eq 18). From the similar relationships seen in Tables VII, and III, VIII and V and eq 18 and 20 it appears that the chosen subset is a realistic representation of the whole. Additionally, it can be noted from Table VIII that C_{50}(A)(T) is not related to C_{50}(G·C) although it is reasonably covariant with C_{50}(A-T).

The ratio $[C_{50}(G\cdot C)]/[C_{50}(A)(T)]$, when employed as an independent variable, provided eq 21. The coefficient

$$\log ILS_{max} = -0.47(\pm 0.35)R_m^2 - 0.28(\pm 0.19)R_m + 0.08(\pm 0.14) \log [[C_{50}(G\text{-}C)]/[C_{50}(A)(T)]] + 2.09 \quad (21)$$

$$n = 41,\ r = 0.62,\ s = 0.21,\ F_{3,37} = 7.8$$

associated with the C_{50} ratio term in eq 21 is not significantly different from zero and provides no improvement over a two-variable equation in R_m and R_m^2 alone.

The equations developed demonstrate clearly that the selective antitumor properties of the bisquaternary salts result from their lipophilic–hydrophilic balance and ability to distinguish certain DNA sites. Further, such sites presumably have an excess of alternating A·T residues and a lesser number of G·C base pairs. These appear to be quite remarkable conclusions to reach from attempted modeling of screening results from intact animal studies.

It is not known if there is a single critical DNA site of action, several, or many. Since there is a residuum of as yet unexplained variance in the screening data, it might prove possible to further delineate the sequence of a single critical site or that of a group of highly complementary sites. If sufficient synthetic DNAs of defined sequence were available, then measurement of the C_{50} values for these, with, for example, the compounds of the subset of Table VI, could be readily carried out. Following regression analysis of these data might allow selection of a synthetic DNA which most closely corresponds in sequence to that of the critical site(s). The preliminary work of this paper provides an indication that such may well be possible. Pinpointing of critical site features, in this fashion, by employing data from animal screening tests, would constitute a novel demonstration of the remarkable power of regression analytical techniques currently available.

Judging from the goodness of fit of the various equations derived for the three measures of biologic activity, ILS_{max}, D_{40}, and CI, it is apparent that ILS_{max} is the superior parameter. It is noteworthy that no significant correlation equation could be derived for LD_{10}. Possibly this reflects the diversity of compounds in the data set and presumably their quite different rates of metabolism and excretion, etc.,

Table VIII. Squared Correlation Matrix for the Independent Variables Associated with the Entries of Table VI

	R_m^2	log $[1/C_{50}(ct)]$	log $[1/C_{50}(A\cdot T)]$	log $[1/C_{50}(G\cdot C)]$	log $[1/C_{50}(A)(T)]$	log $[[C_{50}(G\text{-}C)]/[C_{50}(A)(T)]]$
R_m	0.094	0.154	0.003	0.130	0.015	0.150
R_m^2		0.000	0.001	0.000	0.000	0.000
log $[1/C_{50}(ct)]$			0.468	0.927	0.074	0.332
log $[1/C_{50}(A\text{-}T)]$				0.407	0.684	0.216
log $[1/C_{50}(G\text{-}C)]$					0.039	0.440
log $[1/C_{50}(A)(T)]$						0.360

which will influence what fraction of administered dose will ultimately reach critical sites. It may not then be surprising, in view of the covariance seen between LD_{10} and D_{40} (Table III), that the latter has proved less effective as a measure of biologic activity. Employing the LD_{10} as a constant dose, at which measurement of biologic response is made, must compensate in reasonable measure for the diversion of administered drug by metabolism and other causes.

The ILS_{max} values of most active compounds are reasonably well predicted by eq 15, as are the inactivities of the bulk of those lacking biologic activity. Importantly, markedly divergent examples can be immediately noted by scrutiny of the residuals listed in Table I. Thus, compounds **189–191** comprise a small homologous series wherein activities are quite depressed. These three molecules possess the greatest charge separation of all the compounds in the data base, and it is possible that an upper limit to such separation is being reached. Additionally, the series **251–253** and **254–256** are two where activities are also well depressed. Since both groups contain a common 2″-NH_2 group, it may be surmised that this function is in some way responsible for the depression seen. The inactivity of all 2-substituted pyridinium compounds examined (**206–214**) is not in accord with the predictions of eq 15. It would clearly be of interest to examine the C_{50} values for these less well predicted compounds with a more extensive range of synthetic DNAs.

Intercalating Variants. Compounds **294–298** constitute a small group of highly active compounds which were not included in the derivation of eq 15. Although there is apparently a close relationship to the quinoline quaternary salts (e.g., **290**) in two-dimensional representations of structure, there is one important difference. In progressing from a 4-anilinoquinoline to a 9-anilinoacridine system, steric interactions, stemming from the additional fused ring in the latter, force the plane of the appended 9-anilino ring system well away from that of the acridine ring plane.[29] Bisquaternary salts based on the 9-anilinoacridine system (**294–298**) then do not have, overall, close to planar structures. Representatives of the 4-anilinoquinoline system (**216**, **221**, and **229**) do not remove superhelical turns in bacteriophage PM2 DNA[17] and, to this criterion, are not intercalating agents. However, examples of the acridine bisquaternary salts do provide unwinding of this DNA[17] and can then be classified as intercalating agents. Presumably it is the acridine nucleus of these agents which intercalates into the nucleic acid. These compounds (**294–298**) distinguish between the A·T and G·C polymers to a much greater extent than do the simple 9-anilinoacridines.[15] On the basis of later discussion it can be hypothesized that these agents have the acridine nucleus intercalated into the DNA and the remainder of the molecules lodged in the minor groove. These compounds then act as conceptual bridges between the minor groove binding bisquaternary salts and the extensive series of 9-anilinoacridines (AMSA agents)[30] which bind to DNA predominantly by intercalation.[31] In fact, the genesis of the AMSA series lay in the initial lead provided by the bisquaternary salts, followed through the series of quinoline variants (e.g., **216–293**)[7,8] and a group of dibasic acridines akin to **292–298**.[32]

All the acridine bisquaternary compounds (**294–298**) have exceptional antitumor activity and provide long-term survivors in standard L1210 assays. They are poorly predicted by eq 12, being much more active than expected. Recalculation of eq 12 including these five acridine compounds provides the significantly less well fit eq 22.

$$\log ILS_{max} = -0.37(\pm0.12)R_m^2 - 0.19(\pm0.06)R_m + 0.41(\pm0.07)\log[1/C_{50}(A\cdot T)] - 0.16(\pm0.09)\log[1/C_{50}(G\cdot C)] + 1.90 \quad (22)$$

$$n = 179,\ r = 0.76,\ s = 0.15,\ F_{4,174} = 61.4$$

Addition of an indicator variable denoting the presence ($I = 1$) or absence ($I = 0$) of an acridine ring system provided the improved eq 23. Comparison of eq 12 and

$$\log ILS_{max} = -0.38(\pm0.10)R_m^2 - 0.27(\pm0.09)R_m + 0.42(\pm0.07)\log[1/C_{50}(A\cdot T)] - 0.27(\pm0.09)\log[1/C_{50}(G\cdot C)] + 0.46(\pm0.15)I + 1.88 \quad (23)$$

$$n = 179,\ r = 0.81,\ s = 0.14,\ F_{5,173} = 67.1$$

23 shows these to be virtually identical except for the indicator variable in the latter. To the extent of the small number of acridine compounds available these must follow the same quantitative SAR as the bisquaternary salts, with a log ILS_{max} increment of 0.46 conferred by the acridine system. From the discussion above it is tempting to attribute this considerable increment in activity to the ability of these compounds to intercalate their acridine nuclei into DNA. If the findings embodied in eq 12 are correct, then acridine compounds related to **294–298**, which are better able to distinguish between poly[d(A·T)] and poly[d(G·C)], should possess even greater antitumor selectivity.

Structural Features Modifying C_{50} Values. There is little doubt that a considerable proportion of the binding interaction of the bisquaternary salts with DNA stems from the aromatic ring components. Thus, loss of aromatic rings from **151** to give progressively **112** and **111** results in a progressive increase in C_{50} values [C_{50}(A·T) = 0.41, 7.7, and 63 μM, respectively]. Similarly, compounds with aliphatic link units (**193–196**) have high C_{50} values in comparison with those containing aromatic ring systems in the same relative position (**178–192**). From model fitting, and by considering the likely order of the relative magnitudes of the possible binding forces involved, it can be suggested that the DNA binding contributions provided by the aromatic ring components probably result from ion ($-PO_2^-$)–dipole interactions as well as the associated van der Waals contact forces.

The sequence selectivity of DNA binding, observed with the bisquaternary salts, invariably favors better binding to poly[d(A·T)]. Similar binding distinctions have been observed with distamycin and it has been suggested that there is selective hydrogen-bond formation between polar functions of the drug and the A·T pairs distinguished. However, fitting of space-filling models (Courtald) of the bisquaternary salts to that of twin-helical DNA shows that most of the polar link structures employed in these agents are unlikely to be able to form reasonably dimensioned H bonds with base-pair functionality due to steric limitations imposed by the aromatic ring units employed. The models do, however, show that the observed distinction for poly[d(A·T)] might not result from a positive discrimination for this polymer but rather from an inhibition of binding to poly[d(G·C)]. The models suggest that a dominant steric inhibition of drug binding would be exerted by the 2-NH_2 group of guanine, particularly exacerbated if this function has associated H-bonded water molecule(s). On such steric grounds, the binding distinction between d(A·T) and d(G·C) would depend primarily on how far the skeletal framework between the two charged functions of any drug extended into the minor

groove, thus impinging against the guanine amino groups. For example, in the 3-aminopyridine quaternary salt **151**, when cationic charges are matched to the exterior phosphates of the DNA, the skeletal framework of the agent lies along the outside of the minor groove and is, in consequence, only mildly discriminatory against the G·C polymer [$[C_{50}$(G-C)]/[C_{50}(A-T)] = 2.2]. In a variant utilizing the same skeletal framework but containing highly angular 4-anilinopyridinium basic functions (**178**), similar matching of cationic drug charges to anionic site phosphates results in the drug framework being forced deeper into the minor groove and an apparently high A·T selectivity results [$[C_{50}$(G·C)]/[C_{50}(A-T)] = 12.9]. Such considerations, coupled with judicious model building, appear in qualitative agreement with the A·T/G-C selectivities observed. Quantitative ordering of such results appears a somewhat more formidable task.

If the above views are correct is should prove possible to construct a bisquaternary salt which contains no polar functions capable of H bonding to specific base-pair functionality, yet would demonstrate selectivity of binding to poly[d(A-T)], and, providing it was of suitable lipophilic–hydrophilic balance, should also then prove tumor active. Of the quaternary salt functions investigated, which contain no peripheral H-bond donor or acceptor groups, the *N*-arylpyridinium salts prove the most hydrophilic. A distyryl-linked bisquaternary salt, utilizing this basic function (**299**), has no polar groups which can H bond with base-pair functionality but nevertheless binds selectively to poly[d(A-T)] in relation to poly[d(G·C)] [$[C_{50}$(G-C)]/[C_{50}(A-T)] = 10.5]. From the measured R_m value of **299** and the C_{50} values for poly[d(A-T)] and poly[d(G-C)], it proved possible to predict from eq 15 that this compound would be L1210 active, and the absolute magnitude of such activity was quite reasonably predicted—before the screening in animals was undertaken.

Experimental Section

Melting points were determined in open capillaries on an Electrothermal melting point apparatus with the makers' stem corrected thermometer and are as read. Quaternary salts as crystallized from aqueous solvents are often extensively hydrated. For analysis, samples have been dried in vacuo over silica gel at room temperature. Attempts to dry thoroughly at elevated temperatures gave extremely hygroscopic samples and, in some cases, a loss of crystallinity. Melting points have been determined on the samples dried and ready for analysis.

UV spectra were determined on a Shimadzu UV 200. To monitor the progress of reactions, purification of products, etc., TLC on SiO_2 (Merck SiO_2 F_{254}) was used. Homogeneity of the bisquaternary salts was best monitored by employing the top phase of a mixture of *n*-BuOH–HOAc–H_2O (5:1:4; v/v) as solvent.

R_m Values. The top phase of a mixture of *i*-BuOH, HOAc, H_2O, and DMF (30:6:24:2.25; v/v) was used with Merck DC cellulose F_{254}. Agents were detected by UV scanning and spraying with Dragendorff's reagent. Quaternary salts were applied as solutions in the lower phase of the solvent mixture. Applied spots should not be dried on the cellulose sheets by the application of heat; under such conditions certain quaternary salts appear to complex firmly with the cellulostic support and then fail to move satisfactorily on subsequent development. Immediately after each sheet was spotted, it was transferred to a developing tank whose walls were hung with filter paper soaked in the lower phase of the solvent mixture. An equilibration time of 17 h was employed before development with the top phase. Values are the mean of four determinations. The standard errors found associated with such measurements were normally inside the range of ±0.03.

C_{50} Values. The fluorimetric method, earlier detailed in full,[15,16] was employed with substitution of the requisite nucleic acid for the calf thymus DNA then used. With selected agents multiple determinations of C_{50} values provided figures which have lain within an extreme range of ±9% of the mean value.

6-[4-(Methoxycarbonyl)benzamido]quinoline was prepared by the usual phosphorazo coupling[2] of equimolecular quantities of 6-aminoquinoline and methyl potassium terephthalate[2] in pyridine solution. Pure product (92% yield) separated as colorless needles from DMF–MeOH: mp 222–223 °C. Anal. ($C_{18}H_{14}N_2O_3$) C, H, N. The ester function in the latter was saponified by stirring with excess 1 N KOH in 85% aqueous MeOH until dissolved and then standing at room temperature for a further 1 h. Precipitation from the clarified solution, by addition of a volume of 1 N HCl equivalent to the KOH employed, afforded the corresponding acid as a microcrystalline, TLC homogeneous precipitate.

3-[(4-Nitrophenyl)carbamoyl]pyridine was similarly prepared by phosphorazo coupling of 4-nitroaniline and nicotinic acid. The product crystallized as yellow needles from EtOH: mp 259–260 °C (87% yield). Anal. ($C_{12}H_9N_3O_3$) C, H, N.

3-[(4-Aminophenyl)carbamoyl]pyridine was prepared by Fe/H^+ reduction[2] of the preceding compound and separated from an EtOH–H_2O solution as colorless needles of mp 186–187 °C (83% yield). Anal. ($C_{12}H_{11}N_3O$) C, H, N.

300. Phosphorazo coupling of 6-(4-carboxybenzamido)quinoline and 3-[(4-aminophenyl)carbamoyl]pyridine in dry *N*-methyl-2-pyrrolidone (NMePy)–pyridine solution provided bisbase **300** (Table II) in 71% yield.

3-(3-Nitrobenzamido)pyridine resulted from phosphorazo coupling of 3-nitrobenzoic acid and 3-aminopyridine. Pure product was obtained from EtOH–H_2O as pale yellow needles of mp 149–150 °C. Anal. ($C_{12}H_9N_3O_3 \cdot H_2O$) C, H, N.

3-(3-Aminobenzamido)pyridine was obtained by Fe/H^+ reduction of the aforementioned product and crystallized from EtOH–H_2O as colorless needles of mp 161–162 °C. Anal. ($C_{12}H_{11}N_3O$) C, H, N.

3-[3-[4-(Methoxycarbonyl)benzamido]benzamido]pyridine was prepared by phosphorazo coupling of 3-(3-aminobenzamido)pyridine and methyl potassium terephthalate. Pure product separated from DMF–MeOH solution as colorless needles of mp 231–232 °C (87%). Anal. ($C_{21}H_{17}N_3O_4$) C, H, N.

3-[3-(4-Carboxybenzamido)benzamido]pyridine resulted from saponification of the methyl ester function in the preceding compound, essentially as before, but with added DMF to increase solubility. Pure acid crystallized from DMF–H_2O as colorless needles of mp 325–326 °C. Anal. ($C_{20}H_{15}N_3O_4$) C, H, N.

301. Phosphorazo coupling of the aforementioned acid and 3-(4-aminobenzamido)pyridine[2] in NMePy–pyridine solution provided crude product. Crystallization from DMF–MeOH provided the TLC homogeneous product (72% yield; Table II).

3-(4-Nitro-1-naphthamido)pyridine resulted from standard coupling of 4-nitro-1-naphthoic acid and 3-aminopyridine. Pure product separated from DMF–H_2O as pale yellow crystals of mp 168–169 °C (82%). Anal. ($C_{16}H_{11}N_3O_3 \cdot 0.5H_2O$) C, H, N.

3-(4-Amino-1-naphthamido)pyridine was obtained by Fe/H^+ reduction of the preceding product and crystallized from EtOH–H_2O as colorless needles of mp 203–205 °C (91%). Anal. ($C_{16}H_{13}N_3O \cdot 0.5H_2O$) C, H, N.

302. Phosphorazo coupling of 3-(4-amino-1-naphthamido)-pyridine [dried in a vacuum oven at 120 °C (15 mm)] and 3-[4-(4-carboxybenzamido)benzamido]pyridine provided the desired product which separated from DMF–MeOH as colorless crystals (83% yield; Table II).

307 was prepared by reacting 4-chloro-8-nitroquinoline and 4-[4-(4-aminobenzamido)anilino]pyridine[6] in acid media as before.[6,8] The pure bisbase separated from DMF–H_2O as pale yellow crystals (83% yield; Table II).

309 was similarly prepared in 87% yield by reacting 4-chloro-6-nitro-8-methoxyquinoline and 4-[4-[(4-aminophenyl)-carbamoyl]anilino]pyridine[7] by the standard method. Pure product crystallized readily from DMF–MeOH (Table II).

312 (Table II) resulted from similar interaction of 4-chloro-6-nitroquinoline and 3-[[4-[(4-aminophenyl)carbamoyl]benzamido]benzamido]pyridine.[4]

2-(4-Carboxyphenyl)-1,3-dioxolane. 4-Carboxybenzaldehyde (15.1 g, 0.1 mol) was suspended in C_6H_6 (150 mL) containing ethylene glycol (28 mL) and 4-toluenesulfonic acid hydrate (50 mg), and the mixture was heated to reflux under a Dean-Stark water entrainment head until no further H_2O was removed (2 h). Following removal of C_6H_6 in vacuo a solution of NaOH (8 g) in H_2O (100 mL) was added, and the mixture was warmed until

homogeneous and then allowed to stand at room temperature for 1 h. The latter step saponifies ester functions also generated in the initial condensation. Following cooling of the solution to 0 °C crude product was precipitated by addition of HOAc (12 mL). Product was collected in $CHCl_3$ and the washed (H_2O) and dried (Na_2SO_4) solution evaporated to a small volume. Petroleum ether was then added to turbidity at the boil, and cooling then provided TLC homogeneous product as colorless plates of mp 177–178 °C (11.0 g; 57%). Anal. ($C_{10}H_{10}O_4$) C, H.

2-[[(4-Nitrophenyl)carbamoyl]phenyl]-1,3-dioxolane was prepared by phosphorazo coupling of the preceding product and 4-nitroaniline. Pure product separated as pale yellow needles from DMF–MeOH, mp 267–268 °C (73% yield). Anal. ($C_{16}H_{14}N_2O_5$) C, H, N.

4-[(4-Nitrophenyl)carbamoyl]benzaldehyde. To a suspension of the preceding dioxolane (6.8 g, 0.021 mol) in boiling dioxane (110 mL) was added in one portion 12 N HCl (7.5 mL), the starting material promptly dissolving, and then the desired product crystallized from the solution. Following thorough cooling, product was collected and recrystallized from DMF–H_2O, separating as pale yellow needles of mp 284–286 °C (87%). Anal. ($C_{14}H_{10}N_2O_4$) C, H, N.

2-[4-[(Nitrophenyl)carbamoyl]styryl]-1,4,5,6-tetrahydropyrimidine. The preceding aldehyde (5.42 g, 0.02 mol) was suspended in a mixture of pyridine (20 mL), ethyl formate (20 mL), and DMF (10 mL), then 2-methyl-1,4,5,6-tetrahydropyrimidine (2.5 g, 0.026 mol) added, and the mixture heated on a steam bath for 18 h. After evaporation in vacuo, EtOH (30 mL) and 12 N HCl (3 mL) were added and the solution was reevaporated. The residue was extracted with boiling 0.01 N HCl (660 mL) and NaCl (100 g) dissolved in the hot clarified solution. On cooling, crude product hydrochloride crystallized from the solution. Multiple crystallizations from EtOH–H_2O–HCl provided TLC homogeneous product hydrochloride as colorless needles of mp 328–329 °C (27% yield). Anal. ($C_{19}H_{19}N_4O_3Cl\cdot1.5H_2O$) C, H, N, Cl.

2-[4-[(4-Aminophenyl)carbamoyl]styryl]-1,4,5,6-tetrahydropyrimidine was prepared by Fe/H^+ reduction of the aforementioned product and was conveniently purified as the bishydrochloride: colorless needles from boiling 1 N HCl; mp 339 °C dec (79% yield). Anal. ($C_{19}H_{22}N_4OCl_2\cdot H_2O$) C, H, N, Cl.

1-Methyl-1,4-dihydro-6-nitroquinol-4-one was prepared in 72% yield by the method formerly used to prepare the corresponding 1-ethyl analogue.[7] Pure compound crystallized from pyridine–H_2O as bronze needles of mp 236–237 °C. Anal. ($C_{10}H_8N_2O_3$) C, H, N.

311. 1-Methyl-4-chloro-6-nitroquinolinium chloride was prepared in situ, as before,[7] by the action of $SOCl_2$–DMF on 1-methyl-1,4-dihydro-6-nitroquinol-4-one. This quinolinium salt was reacted with 2-[4-[(4-aminophenyl)carbamoyl]styryl]-1,4,5,6-tetrahydropyrimidine bishydrochloride in 65% EtOH–H_2O solution as before[7] to provide the desired product (Table II).

294. 1-Methyl-4-[4-[(4-aminophenyl)carbamoyl]anilino]-pyridinium bromide[7] (0.02 mol) and 3-(trifluoroacetamido)-9-chloro-10-methylacridinium chloride (0.02 mol) were reacted in 65% aqueous EtOH (125 mL) as before[12] until TLC monitoring demonstrated complete reaction. Following cooling to 25 °C sufficient 12 N NH_3 was added to provide a 4 N concentration and the solution allowed to stand until TLC demonstrated complete removal of the trifluoroacetyl group. Adjusting the pH to below 4 with HCl, removal of EtOH in vacuo, and addition of an equal volume of saturated aqueous NaCl precipitated crude, crystalline **294** chloride salt. Further crystallization from EtOH–H_2O–NaCl provided TLC homogeneous agent (68%) as vermilion-colored needles (Table II).

4-[4-[(4-Nitrophenyl)sulfamoyl]anilino]pyridine was prepared from 4-[(4-nitrophenyl)sulfamoyl]aniline and *N*-pyridyl-4-pyridinium chloride hydrochloride by the methods derived earlier.[4] Pure product crystallized from EtOH–H_2O as yellow prisms of mp 261–262 °C (67% yield). Anal. ($C_{17}H_{14}N_4O_4S$) C, H, N, S.

1-Methyl-4-[4-[(4-nitrophenyl)sulfamoyl]anilino]-pyridinium Chloride. Attempted preparation of this compound by direct quaternization of the preceding product afforded multiple products, presumably due to cooccurring alkylation of the sulfonamide function. Vigorous acetylation, employing refluxing Ac_2O containing NaOAc for 3 h, provided a TLC homogeneous acetyl derivative which crystallized from HOAc. This product, on treatment with 1 N NH_3–EtOH at room temperature, slowly returned the starting sulfonamide; at reflux temperature deprotection was complete in 15 min. To a solution of the above acetyl derivative (18.2 g) in the minimum necessary volume of hot (120 °C) nitrobenzene, methyl *p*-toluenesulfonate (14.9 g) was added in one portion. After 15 min at this temperature the mixture was cooled and the deposited quaternary salt washed with dry *i*-Pr_2O, dried in vacuo, and dissolved in EtOH (75 mL). After addition of 12 N aqueous NH_3 (11 mL) the solution was heated to reflux for 15 min, then solvent removed in vacuo, and 2 N HCl (50 mL) added to the residue. Crude quaternary salt was collected from the cooled mixture and crystallized from boiling 0.01 N HCl until homogeneous to TLC. Pure product was obtained as colorless needles of mp 180–182 °C (11.2 g). Anal. ($C_{18}H_{17}N_4SO_2Cl$) C, H, N, S, Cl.

1-Methyl-4-[4-[(4-aminophenyl)sulfamoyl]anilino]-pyridinium chloride was prepared by Fe/H^+ reduction of the corresponding nitro compound. Pure product (76% yield) separated from H_2O–NaCl as colorless needles of mp 193–195 °C. Anal. ($C_{18}H_{19}N_4SO_2Cl$) C, H, N, S, Cl.

295. Reaction of the preceding product with 3-(trifluoroacetamido)-9-chloro-10-methylacridinium chloride by the standard method and following deprotection with aqueous NH_3 and workup in the usual manner provided crude agent. Crystallization from EtOH–H_2O provided TLC homogeneous product as red needles (76% yield; Table II).

296. 4-[(Aminophenyl)carbamido]acetophenone[7] and 3-[(trifluoroacetyl)amino]-9-chloro-10-methylacridinium chloride were coupled by the standard method, and the protecting trifluoroacetyl function was removed as in earlier examples. The crude chloride salt resulting from this sequence (81%), TLC demonstrating contamination with 3-amino-10-methyl-9(10*H*)-acridone, was dissolved in the minimum necessary volume of boiling 60% EtOH–H_2O which was 2 N in HCl. After addition of a twofold excess of aminoguanidine hydrochloride the solution was heated on a steam bath for 1 h, the desired product crystallizing progressively from the solution. A further crystallization from EtOH–H_2O–NaCl provided TLC homogeneous product (Table II).

N^1-[4-[(4-Nitrophenyl)carbamido]phenyl]biguanide Hydrochloride. 4-[(4-Nitrophenyl)carbamido]aniline (0.019 mol) and dicyanodiamide (0.028 mol) in dry NMePy (35 mL) containing methanesulfonic acid (0.19 mol) were heated together at 140 °C, with stirring, for 20 min. Dilution of the cooled mixture with C_6H_6 (250 mL) precipitated an oil which solidified on trituration with petroleum ether. The dried solid was dissolved in boiling H_2O (550 mL) containing 12 N HCl (1 mL), decolorizing charcoal added, and then hot 20% NaCl–H_2O added to the clarified solution until crystallization initiated. Recrystallization from NaCl–H_2O provided TLC homogeneous product as yellow prisms of mp 241–242 °C (73%). Anal. ($C_{15}H_{17}N_8O_3Cl$) C, H, N, Cl.

297. Fe/H^+ reduction of the preceding nitro compound by the usual method provided a very readily autoxidized amine which rapidly furnished colored oxidation products on exposure to air. Accordingly, following demonstration of homogeneity by TLC and employing minimal further manipulation, this product was immediately coupled with 3-(trifluoroacetamido)-9-chloro-10-methylacridinium chloride, as before. Terminal hydrolytic removal of the trifluoroacetyl group in the usual way provided the desired product (Table II).

1,4-Bis(4-nitrostyryl)benzene has been prepared by a variety of methods[33-35] but moderate quantities can be simply prepared by the following route employing commercially available starting materials. To (4-nitrophenyl)acetic acid (54 g, 0.3 mol) and terephthaldicarboxaldehyde (20.1 g, 0.15 mol) dissolved in NMePy (60 mL) was added piperidine (60 mL), and the resulting mixture was heated on a steam bath for 3 h. C_6H_6 (100 mL) was then added and the mixture heated to reflux (oil bath) under a Dean-Stark H_2O entrainment head for 12 h. Solvent was then distilled until an internal temperature of 160 °C was reached and this temperature maintained for 1 h. Following cooling, MeOH (120 mL) was added and the mixture briefly boiled and then thoroughly cooled. The collected crystals were recrystallized once from DMF–MeOH and then DMF. TLC homogeneous product

was obtained as glistening orange plates of mp 290–291 °C (24% yield). Anal. ($C_{22}H_{16}N_2O_4$) C, H, N. Quoted melting points for this compound are 262–264,[33] 280,[34] and 290 °C.[35]

1,4-Bis(4-aminostyryl)benzene. To the above dinitro compound (8.9 g, 0.024 mol) suspended in boiling HOAc (600 mL) was added a solution of $SnCl_2 \cdot 2H_2O$ (65 g, 0.29 mol) in 12 N HCl (65 mL) and the mixture stirred vigorously while boiling. After ca. 0.5 h of heating a clear solution resulted, and after a further 0.5 h the volume was reduced in vacuo to 90 mL and 12 N HCl (30 mL) added. After thorough cooling the crystals were collected, washed well with saturated brine, and then suspended in a solution of NaOH (45 g) in H_2O (450 mL), and the whole mixture was stirred until of homogeneous consistency. The insoluble diamine was collected, washed well with H_2O, dried, and crystallized from DMF–EtOH. Pure product was obtained as off-white needles of mp 297–298 °C; λ_{max} (20% DMF–EtOH) 385.5 nm (log ϵ 4.71), lower peaks were obscured by the solvent necessary for solution. Anal. ($C_{22}H_{20}N_2$) C, H, N.

299. In the preparation of simple N-substituted pyridines Zincke[13] could employ *N*-(2,4-dinitrophenyl)pyridinium chloride for reaction with primary amines. However, the marked insolubility of this pyridinium chloride in solvents in which 1,4-bis(4-aminostyryl)benzene could be dissolved prevented successful reaction. A simple change of anion, to 4-toluenesulfonate, provided a suitably soluble salt. Addition of excess 20% aqueous sodium 4-toluenesulfonate, acidified to pH below 4 with 4-toluenesulfonic acid, to a saturated aqueous solution of *N*-(2,4-dinitrophenyl)-pyridinium chloride precipitated the required salt. A single crystallization from a small volume of boiling water provided pure ***N*-(2,4-dinitrophenyl)pyridinium 4-toluenesulfonate** as massive prisms of mp 255–257 °C. Anal. ($C_{18}H_{15}N_3O_7S$) C, H, N, S.

A suspension of 1,4-bis(4-aminostyryl)benzene (5 g, 0.016 mol) and *N*-(2,4-dinitrophenyl)pyridinium 4-toluenesulfonate (26.75 g, 0.064 mol) in anhydrous dimethylacetamide (80 mL) was heated while stirring until a solution resulted. The reaction mixture was then boiled for 30 min and cooled, and crude product was precipitated with $CHCl_3$ (375 mL). The solid was washed by alternately suspending in boiling $CHCl_3$ and filtering. This process was continued until all yellow 2,4-dinitroaniline, a further product of the reaction, was completely removed. The solid residue was suspended in H_2O (1100 mL) and the suspension boiled for 15 min, decolorizing charcoal added, and the solution clarified. Overnight cooling of the filtrate provided crystalline product. Further crystallization from H_2O (100 mL/g) and then EtOH–H_2O containing sodium 4-toluenesulfonate provided TLC homogeneous **299** (Table II) as yellow needles (3.35 g; 32%): λ_{max} (H_2O) 372.5 nm (log ϵ 4.79), shoulders at 219 (4.63) and 248 (4.31).

L1210 Screening. The L1210 leukemia was maintained by serial, weekly transfer (10^5 cells ip in DBA_2 mice) for periods of no longer than 3 months. At three monthly intervals tumor was refurbished with a sample withdrawn from liquid N_2 storage.

Antitumor tests were performed in $C_3H♀ \times DBA_2♂$ F_1 hybrid mice produced in the animal colonies of this laboratory. Animals were implanted with 10^5 L1210 cells ip on day 0. Drug treatment was ip once daily on days 1–5. Animal deaths were recorded twice daily. Every attempt was made to obtain solutions of the quaternary salts in H_2O so that the dose for a 20-g mouse was contained in a 0.2-mL volume. Animals in the 18.5–22.5-g weight range were employed but any drug-treated group contained weight matched animals varying by no more than 1 g. No significant difference in the mean life span of groups of control animals within this weight range could be detected. There were a minimum of six animals per treatment group and one control group was employed with every six treatment groups.

A dose–response profile of antileukemic activity was accumulated employing doses separated by 0.09 log dose intervals. In determination of the LD_{10} the doses employed were separated by 0.05 log dose intervals and animals observed for a 50-day period. The LD_{10} dose was derived by linear correlation of percent probit mortalities and the logarithms of the corresponding drug doses employed, as before.[24] Significant life extensions in leukemia L1210 assays, obtained at and below the LD_{10} dose, were linearly correlated with the logarithms of the corresponding doses employed. The percentage increase in life span (ILS) specified by the regression line at the measured LD_{10} dose was employed as ILS_{max}. The dose providing 40% increase in life span in L1210 tests (D_{40}) was also obtained from this regression line.

While the confidence limits on ILS_{max} are not centrosymmetric, those for log ILS_{max} are more nearly so.[24] From the 95% confidence limits about the ILS/log dose regression line and the LD_{10} dose it can be predicted that log ILS_{max} should be duplicable within the limits of ±0.15.[24] Replicate screening by the methods described has provided values within these limits.

Acknowledgment. This work was supported by the Auckland Division of the New Zealand Cancer Society and in part by the Medical Research Council of New Zealand. We are indebted to E. M. Falkenhaug for assistance with the C_{50} determinations and C. West and her assistants for performance of the many biological screening tests.

References and Notes

(1) G. J. Atwell and B. F. Cain, *J. Med. Chem.*, **10**, 706 (1967).
(2) G. J. Atwell and B. F. Cain, *J. Med. Chem.*, **11**, 295 (1968).
(3) G. J. Atwell, B. F. Cain, and R. N. Seelye, *J. Med. Chem.*, **11**, 300 (1968).
(4) G. J. Atwell, B. F. Cain, and R. N. Seelye, *J. Med. Chem.*, **11**, 690 (1968).
(5) B. F. Cain, G. J. Atwell, and R. N. Seelye, *J. Med. Chem.*, **11**, 963 (1968).
(6) B. F. Cain, G. J. Atwell, and R. N. Seelye, *J. Med. Chem.*, **12**, 199 (1969).
(7) G. J. Atwell and B. F. Cain, *J. Med. Chem.*, **16**, 673 (1973).
(8) G. J. Atwell and B. F. Cain, *J. Med. Chem.*, **17**, 930 (1974).
(9) B. F. Cain and G. J. Atwell, *J. Med. Chem.*, **19**, 1417 (1976).
(10) W. Foerst, Ed., "Newer Methods of Preparative Organic Chemistry", Vol. 2, Academic Press, New York, NY, 1963.
(11) L. F. Fieser and M. Fieser, "Reagents for Organic Synthesis", Vol. 1, Wiley, New York and London, 1967, p 371.
(12) B. F. Cain, G. J. Atwell, and W. A. Denny, *J. Med. Chem.*, **19**, 772 (1976).
(13) T. Zincke, *Justus Liebigs Ann. Chem.*, **330**, 361 (1903); **333**, 296 (1904); **338**, 107 (1905); **341**, 365 (1905).
(14) C. Hansch, *Chem. Rev.*, **71**, 525 (1971).
(15) B. F. Cain, B. C. Baguley, and W. A. Denny, *J. Med. Chem.*, **21**, 658 (1978).
(16) B. C. Baguley and E. M. Falkenhaug, *Nucleic Acids Res.*, **5**, 161 (1978).
(17) A. W. Braithwaite, thesis in partial fulfillment for the degree of Master of Science, University of Auckland, 1978.
(18) Leading references may be gleaned from J. D. Watson, Ed., in "The Molecular Biology of the Gene", 3rd ed, W. A. Benjamin, Menlo Park, Ca, 1976.
(19) B. C. Baguley, unpublished observations.
(20) W. Fuller and M. J. Waring, *Ber. Bunsenges. Phys. Chem.*, **68**, 805 (1964).
(21) J. D. McGhee and P. H. Von Hippel, *J. Mol. Biol.*, **86**, 469 (1974).
(22) C. Zimmer, *Prog. Nucleic Acid Res. Mol. Biol.*, **15**, 304 (1975).
(23) M. S. Tute, *Adv. Drug Res.*, **6**, 1 (1971).
(24) W. A. Denny and B. F. Cain, *J. Med. Chem.*, **21**, 430 (1978).
(25) B. F. Cain and W. A. Denny, *J. Med. Chem.*, **20**, 515 (1977).
(26) C. Hansch in "Structure–Activity Relationships", Vol. 1, C. J. Cavallito, Ed., Pergamon Press, Oxford and New York, 1973, p 119.
(27) T. Fujita, *Adv. Chem. Ser.*, **No. 114**, 1 (1972).
(28) W. P. Purcell, G. E. Bass, and J. M. Clayton, Eds., "Strategy in Drug Design", Wiley, New York and London, 1973.
(29) D. Hall, D. A. Swann, and T. N. Waters, *J. Chem. Soc., Perkin Trans. 2*, 1334 (1974).
(30) See W. A. Denny, G. J. Atwell, and B. F. Cain, *J. Med. Chem.*, **20**, 1242 (1977), and earlier references quoted therein.
(31) M. J. Waring, *Eur. J. Cancer*, **12**, 995 (1976).
(32) B. F. Cain, G. J. Atwell, and R. N. Seelye, *J. Med. Chem.*, **14**, 311 (1971).
(33) G. P. Schiemenz and J. Thobe, *Chem. Ber.*, **99**, 2663 (1966).
(34) W. Stilz and H. Pommer, German Patent 1 108 219 (1959); *Chem. Abstr.*, **57**, 732g (1962).
(35) L. V. Shubina and L. Ya. Malkes, *Zh. Org. Khim.*, **1**, 1040 (1965).